# Comparison of Excessive Balmer $\alpha$ Line Broadening of Inductively and Capacitively Coupled RF, Microwave, and Glow Discharge Hydrogen Plasmas with Certain Catalysts

R. L. Mills, P. Ray, E. Dayalan, X. Chen, R. Mayo, J. He, B. Dhandapani,
BlackLight Power, Inc.
493 Old Trenton Road
Cranbury, NJ 08512

ABSTRACT

From the width of the 656.3 nm Balmer $\alpha$ line emitted from inductively and capacitively coupled RF, microwave, and glow discharge plasmas, it was found that inductively coupled RF helium-hydrogen and argon-hydrogen plasmas showed extraordinary broadening corresponding to an average hydrogen atom temperature of $250-310\ eV$ and $180-230\ eV$, respectively, compared to $30-40\ eV$ and $50-60\ eV$, respectively, for the corresponding capacitively coupled plasmas. Microwave helium-hydrogen and argon-hydrogen plasmas showed significant broadening corresponding to an average hydrogen atom temperature of $180-210\ eV$ and $110-130\ eV$, respectively. The corresponding results from the glow discharge plasmas were $33-38\ eV$ and $30-35\ eV$, respectively, compared to $\approx 4\ eV$ for plasmas of pure hydrogen, neon-hydrogen, and xenon-hydrogen maintained in any of the sources. Similarly, the average electron temperatures $T_e$ for helium-hydrogen and argon-hydrogen inductively coupled RF and microwave plasmas were high, $39{,}600 \pm 5\%\ K$, $15{,}800 \pm 5\%\ K$, $28{,}000 \pm 5\%\ K$, and $11{,}600 \pm 5\%\ K$, respectively; compared to $7590 \pm 5\%\ K$, $6000 \pm 5\%\ K$, $6500 \pm 5\%\ K$, and $5500 \pm 5\%\ K$ for the corresponding plasmas of xenon-hydrogen and hydrogen alone, respectively. Stark broadening or acceleration of charged species due to high electric fields can not explain the inductively coupled RF and microwave results since the electron density was low and no high field was present. Rather, a resonant energy transfer mechanism is proposed.

Key Words: RF plasma, microwave plasma, glow discharge plasma, significant line broadening, electron temperature, resonant energy transfer mechanism

# I. INTRODUCTION

Glow discharge devices have been developed over decades as light sources, ionization sources for mass spectroscopy, excitation sources for optical spectroscopy, and sources of ions for surface etching and chemistry [1-3]. A Grimm-type glow discharge is a well established excitation source for the analysis of conducting solid samples by optical emission spectroscopy [4-6]. Despite extensive performance characterizations, data was lacking on the plasma parameters of these devices. M. Kuraica and N. Konjevic [7] and Videnovic et al. [8] have characterized these plasmas by determining the excited hydrogen atom concentrations and energies from measurements of the line broadening of the 656.3 nm Balmer $\alpha$ line. The data was analyzed in terms of Stark and Doppler effects wherein acceleration of charges such as $H^+$, $H_2^+$, and $H_3^+$ in the high fields (e. g. over $10\,kV/cm$) which were present in the cathode fall region was used to explain the Doppler component.

More recently, microhollow glow discharges have been spectroscopically studied as candidates for the development of an intense monochromatic extreme ultraviolet (EUV) light source (e.g. Lyman $\alpha$ ) for short wavelength lithograph for production of the next generation of integrated circuits. A neon-hydrogen microhollow cathode glow discharge has been proposed as a source of predominantly Lyman $\alpha$ radiation. Kurunczi, Shah, and Becker [9] observed intense emission of Lyman $\alpha$ and Lyman $\beta$ radiation at 121.6 nm and 102.5 nm, respectively, from microhollow cathode discharges in high-pressure Ne (740 Torr) with the addition of a small amount of hydrogen (up to 3 Torr). With essentially no molecular emission observed, Kurunczi et al. attributed the anomalous Lyman $\alpha$ emission to the near-resonant energy transfer between the $Ne_2^*$ excimer and $H_2$ which leads to formation of $H(n=2)$ atoms, and attributed the Lyman $\beta$ emission to the near-resonant energy transfer between excited $Ne^*$ atoms (or vibrationally excited neon excimer molecules) and $H_2$ which leads to formation of $H(n=3)$ atoms. Despite the emission characterization of this source, data is lacking about plasma parameters.

For analyses of solids, direct current (DC) glow discharge sources have been successfully complemented by radio-frequency (RF)

discharges [10]. The use of DC discharges is limited to metals; whereas, RF discharges are applicable to non-conducting materials. Other developed sources that provide a usefully intense plasma are synchrotron devices, inductively coupled plasma generators [11], and magnetically confined plasmas. Plasma characterization data on these sources is also limited.

A new chemically generated or assisted plasma source has been developed that is based on a resonant energy transfer mechanism (rt-plasma). One such source operates by incandescently heating a hydrogen dissociator and a catalyst to provide atomic hydrogen and gaseous catalyst, respectively, such that the catalyst reacts with the atomic hydrogen to produce a plasma. It was extraordinary, that intense EUV emission was observed by Mills et al. [12-19] at low temperatures (e.g. $\approx 10^3\ K$) from atomic hydrogen and certain atomized elements or certain gaseous ions which singly or multiply ionize at integer multiples of the potential energy of atomic hydrogen, $27.2\ eV$ that comprise catalysts. The only pure elements that were observed to emit EUV were those wherein the ionization of $t$ electrons from an atom to a continuum energy level is such that the sum of the ionization energies of the $t$ electrons is approximately $m \cdot 27.2\ eV$ where $t$ and $m$ are each an integer.

Since $Ar^+$, $He^+$, and strontium each ionize at an integer multiple of the potential energy of atomic hydrogen, a discharge with one or more of these species present with hydrogen is anticipated to form an rt-plasma. The plasma forms by a resonance transfer mechanism involving the species providing a net enthalpy of a multiple of $27.2\ eV$ and atomic hydrogen.

Mills and Nansteel [14, 19] have reported that strontium atoms each ionize at an integer multiple of the potential energy of atomic hydrogen and caused emission. (The enthalpy of ionization of $Sr$ to $Sr^{5+}$ has a net enthalpy of reaction of $188.2\ eV$, which is equivalent to $m = 7$.) The emission intensity of the plasma generated by atomic strontium increased significantly with the introduction of argon gas only when $Ar^+$ emission was observed. Whereas, no emission was observed when chemically similar atoms that do not ionize at integer multiples of the potential energy of atomic hydrogen (sodium, magnesium, or barium) replaced strontium with hydrogen, hydrogen-argon mixtures, or

strontium alone.

Mills and Nanstell [14, 19] measured the power balance of a gas cell having vaporized strontium and atomized hydrogen from pure hydrogen or argon-hydrogen mixture (77/23%) by integrating the total light output corrected for spectrometer system response and energy over the visible range. Hydrogen control cell experiments were identical except that sodium, magnesium, or barium replaced strontium. In the case of hydrogen-sodium, hydrogen-magnesium, and hydrogen-barium mixtures, 4000, 7000, and 6500 times the power of the hydrogen-strontium mixture was required, respectively, in order to achieve that same optically measured light output power. With the addition of argon to the hydrogen-strontium plasma, the power required to achieve that same optically measured light output power was reduced by a factor of about two. The power required to maintain a plasma of equivalent optical brightness with strontium atoms present was 8600 and 6300 times less than that required for argon-hydrogen and argon control, respectively. A plasma formed at a cell voltage of about 250 V for hydrogen alone and sodium-hydrogen mixtures, 140-150 V for hydrogen-magnesium and hydrogen-barium mixtures, 224 V for an argon-hydrogen mixture, and 190 V for argon alone; whereas, a plasma formed for hydrogen-strontium mixtures and argon-hydrogen-strontium mixtures at extremely low voltages of about 2 V and 6.6 V, respectively.

It was reported [13] that characteristic emission was observed from a continuum state of $Ar^{2+}$ which confirmed the resonant nonradiative energy transfer of $27.2\,eV$ from atomic hydrogen $Ar^{+}$. The transfer of $27.2\,eV$ from atomic hydrogen to $Ar^{+}$ in the presence of a electric weak field resulted in its excitation to a continuum state. Then, the energy for the transition from essentially the $Ar^{2+}$ state to the lowest state of $Ar^{+}$ was predicted to give a broad continuum radiation in the region of $45.6\,nm$. This broad continuum emission was observed. This emission was dramatically different from that given by an argon microwave plasma wherein the entire Rydberg series of lines of $Ar^{+}$ was observed with a discontinuity of the series at the limit of the ionization energy of $Ar^{+}$ to $Ar^{2+}$. The observed $Ar^{+}$ continuum in the region of $45.6\,nm$ confirmed the rt-plasma mechanism of the excessively bright, extraordinarily low voltage discharge. With $Ar^{+}$ as the catalyst, the product hydride ion was

predicted to have a binding energy of $3.05\,eV$, and it was observed spectroscopically at $407\,nm$ [13].

$He^+$ ionizes at $54.417\,eV$ which is $2 \cdot 27.2\,eV$, and novel EUV emission lines were observed from microwave and glow discharges of helium with 2% hydrogen [20]. The observed energies were $q \cdot 13.6\,eV$ ($q = 1,2,3,4,6,7,8,9,$ *or* $11$) or these energies less $21.2\,eV$ due to inelastic scattering of the lines by helium atoms in the excitation of $He\,(1s^2)$ to $He\,(1s^1 2p^1)$. These lines can be explained by the resonance transfer of $m \cdot 27.2\,eV$ [20].

It was anticipated that glow, microwave, and RF discharges would also provide atomic hydrogen and catalyst to form an rt-plasma. To further characterize the plasma parameters observed in rt-plasmas and to study the difference between glow, microwave, and inductively and capacitively coupled RF discharge sources, 1.) the line broadening of the 656.3 nm Balmer $\alpha$ line was measured to determine the excited hydrogen atom energy and concentration in plasmas of hydrogen and a catalyst or plasmas comprising hydrogen with chemically similar controls that did not provide gaseous atoms or ions having electron ionization energies which are a multiple of $27.2\,eV$, and 2.) the electron temperature $T_e$ was measured on microwave and inductively coupled RF plasmas using the ratio of the intensity $I$ of two noble gas lines in two quantum states such as the ratio $I(He\ 501.6\ nm\ line)/\ I(He\ 492.2\ nm\ line)$ and the ratio $I(Ar\ 104.8\ nm\ line)/\ I(Ar\ 420.06\ nm\ line)$ for plasmas having helium and argon, respectively, alone or as a mixture with hydrogen.

## II. EXPERIMENTAL

### A. Measurement of hydrogen atom temperature and number density from Balmer $\alpha$ line broadening

The Doppler-broadened line shape for atomic hydrogen has been studied on many sources such as hollow cathode [8, 21] and RF [22-23] discharges. The method of Videnovic et al. [8] was used to calculate the energetic hydrogen atom densities and energies from the width of the 656.3 nm Balmer $\alpha$ line emitted from glow, microwave, and inductively and capacitively coupled RF discharge plasmas. Gigosos et al. [24] have

reviewed the literature and have discussed this method. The full half-width $\Delta\lambda_G$ of each Gaussian results from the Doppler ($\Delta\lambda_D$) and instrumental ($\Delta\lambda_I$) half-widths:

$$\Delta\lambda_G = \sqrt{\Delta\lambda_D^2 + \Delta\lambda_I^2} \quad (1)$$

$\Delta\lambda_I$ in our experiments was $\pm 0.025\,nm$ in the case of the glow discharge cells and $\pm 0.006\,nm$ otherwise. The temperature was calculated from the Doppler half-width using the formula:

$$\Delta\lambda_D = 7.16\,X\,10^{-7}\lambda_0\left(\frac{T}{\mu}\right)^{1/2} \quad (nm) \quad (2)$$

where $\lambda_0$ is the line wavelength in nm, $T$ is the temperature in K ($1\,eV = 11{,}605\,K$), and $\mu$ is the molecular weight (=1 for hydrogen). In each case, the average Doppler half-width that was not appreciably changed with pressure varied by ±5% corresponding to an error in the energy of ±5%. The corresponding number densities for noble gas-hydrogen mixtures varied by ±20% depending on the pressure.

### a. Balmer $\alpha$ line broadening recorded on glow discharge plasmas

The width of the 656.3 nm Balmer $\alpha$ line emitted from gas discharge plasmas having atomized hydrogen from pure hydrogen alone and a mixture of 10% hydrogen and helium, argon, neon, or xenon was measured with a high resolution visible spectrometer with a resolution of $\pm 0.025\,nm$ over the spectral range $190 - 860\,nm$. Krypton was not studied due to interference by a KrII line (656.1007 nm) [25] in the region of the Balmer $\alpha$ line. The plasmas were maintained in the cylindrical stainless steel gas cell shown in Figure 1.

The 304-stainless steel cylindrical cell was 9.21 cm in diameter and 14.5 cm in height. The base of the cell contained a welded-in stainless steel thermocouple well (1 cm OD) which housed a thermocouple probe in the cell interior approximately 2 cm from the discharge and 2 cm from the cell axis. At the middle height of the cell wall was a welded-flush stainless steel tube (0.95 cm diameter) which was connected to a flexible stainless steel tube (100 cm in length) that served as a vacuum line from the cell and the line to supply the test gas. The top end of the cell was welded to a high vacuum 11.75 cm diameter conflat flange. A silver

plated copper gasket was placed between a mating flange and the cell flange. The two flanges were clamped together with 10 circumferential bolts. The mating flange contained two penetrations comprising 1.) a stainless steel thermocouple well (1 cm OD) also housing a thermocouple probe in the cell interior approximately 2 cm from the discharge and 2 cm from the cell axis and 2.) a centered high voltage feedthrough which transmitted the power, supplied through a power connector, to a hollow cathode inside the cell.

The axial hollow cathode glow discharge electrode assembly comprised a stainless steel plate (42 mm diameter, 0.9 mm thick) anode and a circumferential stainless steel cylindrical frame (5.08 cm OD, 7.2 cm long) perforated with evenly spaced 1 cm diameter holes. The cathode was attached to the cell body by a stainless steel wire, and the cell body was grounded.

A 1.6 mm thick UV-grade sapphire window with 1.5 cm view diameter provided a visible light path from inside the cell. The viewing direction was normal to the cell axis.

The cell was evacuated with a turbo vacuum pump to a pressure of 4 mtorr. The gas was ultrahigh purity hydrogen or noble gas-hydrogen mixture (90/10%) at 2 torr total pressure. The pressure of each test gas comprising a mixture with 10% hydrogen was determined by adding the pure noble gas to a given pressure and increasing the pressure with hydrogen gas to a final pressure. The partial pressure of the hydrogen gas was given by the incremental increase in total gas pressure monitored by a 0-10 torr absolute pressure gauge. The discharge was carried out under static gas conditions. The discharge was started and maintained by a DC electric field supplied by a constant voltage DC power supply at 275 V which produced a current of about 0.2 A. In the case of helium-hydrogen and argon-hydrogen plasmas, the voltage was increased at 50 V increments from 275 V to 475 V, and the high resolution visible spectra were recorded to observe the effect of voltage on the Balmer $\alpha$ line broadening.

Balmer $\alpha$ line broadening was measured at Jobin Yvon Horiba, Inc, Edison, NJ. The plasma emission from the glow discharges of pure hydrogen and noble gas-hydrogen mixtures was fiber-optically coupled through a 220F matching fiber adapter to a TRIAX 550 Spectrometer

with a standard PMT detector that had a resolution of $\pm 0.025\,nm$ over the spectral range $190\text{-}860\,nm$. The entrance and exit slits were set to $20\,\mu m$. The spectrometer was scanned between $656\text{-}657\,nm$ using a $0.01\,nm$ step size. The signal was recorded by a PMT (Hamamatsu R928) with a stand alone high voltage power supply (950 V) and an acquisition controller (SpectrAcq 2). The data was obtained in a single accumulation with a 1 second integration time.

### b. Balmer $\alpha$ line broadening recorded on microwave discharge plasmas

The width of the 656.3 nm Balmer $\alpha$ line emitted from microwave discharges of pure hydrogen alone and a mixture of 10% hydrogen and helium, argon, neon, or xenon was measured with a high resolution visible spectrometer. The plasmas were maintained in the microwave discharge cell light source shown in Figure 2. Each gas was ultrahigh pure. Each pure test gas or mixture was flowed through a half inch diameter quartz tube at 300 mTorr maintained with a noble gas flow rate of 9.3 sccm or an noble gas flow rate of 8.3 sccm and a hydrogen flow rate of 1 sccm. Each gas flow was controlled by a 0-20 sccm range mass flow controller (MKS 1179A21CS1BB) with a readout (MKS type 246). The cell pressure was monitored by a 0-10 Torr MKS Baratron absolute pressure gauge. The tube was fitted with an Opthos coaxial microwave cavity (Evenson cavity). The microwave generator shown in Figure 2 was an Opthos model MPG-4M generator (Frequency: 2450 MHz). The input power to the plasma was set at 40 watts with forced air cooling of the cell. The microwave cavity was tuned such that the reflected power was less than 2 W. In separate experiments, the power was increased up to 100 W to determine the relationship between input power and Balmer $\alpha$ line broadening.

The plasma emission was fiber-optically coupled through a 220F matching fiber adapter positioned 2 cm from the cell wall to a high resolution visible spectrometer with a resolution of $\pm 0.006\,nm$ over the spectral range $190\text{-}860\,nm$. The spectrometer was a Jobin Yvon Horiba 1250 M with 2400 groves/mm ion-etched holographic diffraction grating. The entrance and exit slits were set to $20\,\mu m$. The spectrometer was

scanned between 655.5-657 *nm* using a 0.005 *nm* step size. The signal was recorded by a PMT with a stand alone high voltage power supply (950 V) and an acquisition controller. The data was obtained in a single accumulation with a 1 second integration time.

### c. Balmer $\alpha$ line broadening recorded on capacitively coupled RF discharge plasmas

The width of the 656.3 nm Balmer $\alpha$ line emitted from capacitively coupled RF discharges of pure hydrogen alone and a mixture of 10% hydrogen and helium, argon, neon, or xenon was measured with a high resolution visible spectrometer. The experimental set up shown in Figure 3 comprised a Pyrex cell reactor (38 cm in length and 13 cm ID) with a diode configuration in which the plasma was confined between two parallel circular stainless steel electrodes (0.1 mm thick X 7.6 cm diameter with a 2 cm separation). For spectroscopic measurements on the plasma emission, a 1 cm diameter quartz window was located in the Pyrex cell wall at the center of the gap between the electrodes. At each end of the cell, a Pyrex cap sealed to the cell with a Viton O ring and a C-clamp. One cap incorporated ports for gas inlet and cathode feedthrough. The other cap incorporated ports for gas outlet and anode feedthrough. The cathode was connected to an 13.56 MHz RF generator (RF VII, Inc., Model MN 500) with a matching network (RF Power Products, Inc., Model RF 5S, 300 W). The input power was 60 W, and the reflected power was less than 1 W. In separate experiments, the power was varied from 40 to 100 W to determine the relationship between input power and Balmer $\alpha$ line broadening.

The cell was operated under gas flow conditions while maintaining a constant gas pressure in the cell. Each gas was ultrahigh purity. The gas pressure inside the cell was maintained at about 300 mTorr with a hydrogen flow rate of 5.5 sccm or an argon flow rate of 5.2 sccm and a hydrogen flow rate of 0.3 sccm. Each gas flow was controlled by a 0-20 sccm range mass flow controller (MKS 1179A21CS1BB) with a readout (MKS type 246). The cell pressure was monitored by a 0-10 torr MKS Baratron absolute pressure gauge. The Balmer $\alpha$ line was recorded on the plasma emission as described in Sec. IIAb.

### d. Balmer $\alpha$ line broadening recorded on inductively coupled RF discharge plasmas

The width of the 656.3 nm Balmer $\alpha$ line emitted from inductively coupled RF discharges of pure hydrogen alone and a mixture of 10% hydrogen and helium, argon, neon, or xenon was measured with a high resolution visible spectrometer. The plasma were maintained in the inductively coupled RF discharge gas cell light source shown in Figure 4. A quartz cell which was 500 mm in length and 50 mm in diameter served as the plasma reactor. A Pyrex cap sealed to the quartz cell with a Viton O ring and a C-clamp incorporated ports for gas inlet, outlet, and photon detection. An unterminated, nine-turn, 17 cm long helical coil (18 gauge magnet wire) wrapped around the outside of the cell was connected to an 13.56 MHz RF generator (RF VII, Inc., Model MN 500) with a matching network (RF Power Products, Inc., Model RF 5S, 300 W). The coil inductance and resistance were 4.7 $\mu H$ and 0.106 $\Omega$, respectively. The coil impedance was 400 $\Omega$ at 13.56 MHz. The input power was 60 W, and the reflected power was less than 1 W. In separate experiments, the power was varied from 40 to 100 W to determine the relationship between input power and Balmer $\alpha$ line broadening.

The cell was operated under gas flow conditions while maintaining a constant gas pressure in the cell. Each gas was ultrahigh purity. The gas pressure inside the cell was maintained at about 300 mTorr with a hydrogen flow rate of 5.5 sccm or an argon flow rate of 5.2 sccm and a hydrogen flow rate of 0.3 sccm. Each gas flow was controlled by a 0-20 sccm range mass flow controller (MKS 1179A21CS1BB) with a readout (MKS type 246). The cell pressure was monitored by a 0-10 torr MKS Baratron absolute pressure gauge. The Balmer $\alpha$ line was recorded on the plasma emission as described in Sec. IIAb.

## B. Electron temperature $T_e$ measurements of microwave and inductively coupled RF discharge plasmas

$T_e$ was measured on microwave and inductively coupled RF plasmas of hydrogen, helium, argon, neon, or xenon alone and each noble gas with

10% hydrogen. The most commonly used spectroscopic diagnostic method to determine the electron temperature $T_e$ of laboratory plasmas is based on determining the relative intensities of two spectral lines as described by Griem [26]. It may be shown that for two emission lines at wavelengths $\lambda_A$ and $\lambda_B$

$$\frac{I_A}{I_B} = \frac{(\sigma g_2 A_{21})_A}{(\sigma g_2 A_{21})_B} e^{-\frac{(E_{2A} - E_{2B})}{kT_e}} \tag{3}$$

where $I_A$ and $I_B$ are the intensities measured at $\lambda_A$ and $\lambda_B$, and $\sigma \propto n^4$ for atomic hydrogen where $n$ is the principal quantum number. The frequency $\nu$, the transition probability $A$, the degeneracy $g$, and the upper level $E$ are known constants from which $T_e$ was determined.

$T_e$ was measured on plasmas of helium alone and helium-hydrogen mixture (90/10%) from the ratio of the intensity of the *He* 501.6 nm (upper quantum level $n=3$) line to that of the *He* 492.2 nm ($n=4$) line. $T_e$ was measured on plasmas of argon alone and argon-hydrogen mixture (90/10%) from the ratio of the intensity of the *Ar* 104.8 nm (upper quantum level $n=3$) line to that of the *Ar* 420.06 nm ($n=4$) line. $T_e$ was also measured by the same method on plasmas of neon or xenon alone or with 10% hydrogen using the ratio of the intensities of two noble gas lines in two quantum states. $T_e$ was measured on plasmas of hydrogen using the ratio of the intensities of two Lyman lines.

To determine the electron temperature, EUV spectroscopy was recorded. The experimental set up comprising a microwave or a inductively coupled RF discharge gas cell light source and an EUV spectrometer which was differentially pumped are shown in Figures 2 and 4, respectively. Due to the extremely short wavelength of this radiation, "transparent" optics do not exist. Therefore, a windowless arrangement was used wherein the microwave or RF discharge cell was connected to the same vacuum vessel as the grating and detectors of the EUV spectrometer. Differential pumping permitted a high pressure in the cell as compared to that in the spectrometer. This was achieved by pumping on the cell outlet and pumping on the grating side of the collimator that served as a pin-hole inlet to the optics. The spectrometer was continuously evacuated to $10^{-4} - 10^{-6}$ torr by a turbomolecular pump with the pressure read by a cold cathode pressure gauge. The EUV

spectrometer was connected to the cell light source with a 1.5 mm X 5 mm collimator which provided a light path to the slits of the EUV spectrometer. The collimator also served as a flow constrictor of gas from the cell. The cell was operated under gas flow conditions while maintaining a constant gas pressure in the cell.

The microwave and the inductively coupled RF plasma cell were run under the conditions given in Secs. IIAb and IIAd, respectively. For spectral measurement, the light emission from each plasma was introduced to a normal incidence McPherson 0.2 meter monochromator (Model 302, Seya-Namioka type) equipped with a 1200 lines/mm holographic grating with a platinum coating. The wavelength region covered by the monochromator was $5-560\,nm$. The UV spectrum ($100-170\,nm$) of the cell emission was recorded with a photomultiplier tube (PMT) and a sodium salicylate scintillator. The PMT (Model R1527P, Hamamatsu) used has a spectral response in the range of $185-680\,nm$ with a peak efficiency at about $400\,nm$. The scan interval was $0.1\,nm$, and the dwell time was $500\,ms$. The inlet and outlet slit were $300\,\mu m$ with a corresponding wavelength resolution of $1\,nm$ (FWHM). The spectra were repeated five times per experiment and were found to be reproducible within less than ±5%.

The electron density was determined using a Langmuir probe according to the method given previously [27].

## III. RESULTS AND DISCUSSION

### A. Balmer $\alpha$ line broadening recorded on glow discharge plasmas

The 656.3 nm Balmer $\alpha$ line width was measured glow discharge light sources normal to the applied electric field direction with a high resolution ($\pm 0.025\,nm$) visible spectrometer. The discharge was started and maintained at 2 Torr total pressure by a DC electric field supplied by a constant voltage DC power supply at 275 V which produced a current of about 0.2 A. The 656.3 nm Balmer $\alpha$ line width recorded on glow discharge plasmas of hydrogen compared with each of xenon-hydrogen (90/10%) and argon-hydrogen (90/10%) are shown in Figures 5 and 6,

respectively. The energetic hydrogen atom densities and energies of the plasmas of hydrogen alone and hydrogen-noble gas mixtures were calculated using the method of Videnovic et al. [8] and are given in Table 1. It was found that helium-hydrogen and argon-hydrogen showed significant broadening corresponding to an average hydrogen atom temperature of $30\text{-}38\,eV$ and an atom density of $3\,X\,10^{13} \pm 20\%\ atoms/cm^3$; whereas, pure hydrogen, neon-hydrogen, and xenon-hydrogen showed no excessive broadening corresponding to an average hydrogen atom temperature of $\approx 4\,eV$. The maximum atom density of only $5\,X\,10^{13} \pm 20\%\ atoms/cm^3$ was observed with pure hydrogen as the test gas even though 10 times more hydrogen was present. No voltage or power effect was observed with the helium-hydrogen or argon-hydrogen plasmas over the range studied.

### B. Balmer $\alpha$ line broadening and $T_e$ measurements recorded on microwave discharge plasmas

The 656.3 nm Balmer $\alpha$ line width recorded with a high resolution ($\pm 0.006\,nm$) visible spectrometer on microwave discharge plasmas of hydrogen compared with each of xenon-hydrogen (90/10%) and helium-hydrogen (90/10%) are shown in Figures 7 and 8, respectively. The statistical curve fit of the hydrogen plasma and the argon-hydrogen plasma emission are shown in Figures 9 and 10, respectively. In each case, the data matched a Gaussian profile having the $X^2$ and R values given in Figures 9 and 10. The energetic hydrogen atom densities and energies of plasmas of hydrogen alone and noble gas-hydrogen mixtures were calculated using the method of Videnovic et al. [8] and are given in Table 2. It was found that the helium-hydrogen and argon-hydrogen microwave plasmas showed extraordinary broadening corresponding to an average hydrogen atom temperature of $180\text{-}210\,eV$ and $110\text{-}130\,eV$, respectively, and an atom density of $4.8\,X\,10^{14} \pm 20\%\ atoms/cm^3$ and $3.5\,X\,10^{14} \pm 20\%\ atoms/cm^3$, respectively. Whereas, pure hydrogen, neon-hydrogen, and xenon-hydrogen showed no excessive broadening corresponding to an average hydrogen atom temperature of $\approx 4\,eV$. The maximum atom density of only $7\,X\,10^{13} \pm 20\%\ atoms/cm^3$ was observed with pure hydrogen as the test gas even though 10 times more hydrogen was

present.

These studies demonstrate excessive line broadening in the absence of an observable effect attributable to an electric field since the hydrogen emission shows no broadening. The broadening as found not to depend on the input power over the range studied.

The results of the $T_e$ measurements on microwave plasmas of pure hydrogen alone and a mixture of 10% hydrogen and helium, neon, argon, or xenon are given in Table 2. Similarly to the ion measurement, the average electron temperatures of helium-hydrogen and argon-hydrogen plasmas were high, $28{,}000 \pm 5\%\ K$ and $11{,}600 \pm 5\%\ K$, respectively. Whereas, the corresponding temperatures of xenon-hydrogen and hydrogen alone plasmas were only $6500 \pm 5\%\ K$, and $5500 \pm 5\%\ K$, respectively.

We have assumed that Doppler broadening due to thermal motion was the dominant source to the extent that other sources may be neglected. To confirm this assumption, each source is now considered. In general, the experimental profile is a convolution of two Doppler profiles, an instrumental profile, the natural (lifetime) profile, Stark profiles, Van der Waals profiles, a resonance profile, and fine structure. The instrumental half-width is measured to be $\pm 0.006\ nm$. The natural half-width of the Balmer $\alpha$ line given by Djurovic and Roberts [22] is $1.4\ X\ 10^{-4}\ nm$ which is negligible. The fine structure splitting is also negligible.

With conventional emission or absorption spectroscopy, Stark broadening of hydrogen lines in plasmas can not be measured at low electron densities because it is hidden by Doppler broadening. For the Lyman $\alpha$ line, the Stark width is larger than the Doppler width only at $n_e > 10^{17}\ cm^{-3}$ for temperatures of about $10^4$ K [28].

The relationship between the Stark broadening $\Delta\lambda_S$ of the Balmer $\beta$ line in nm, the electron density $n_e$ in $m^{-3}$, and the electron temperature $T_e$ in K is

$$\log n_e = C_0 + C_1 \log(\Delta\lambda_S) + C_2[\log(\Delta\lambda_S)]^2 + C_3 \log(T_e) \qquad (4)$$

where $C_0 = 22.578$, $C_1 = 1.478$, $C_2 = -0.144$, and $C_3 = 0.1265$ [29]. From Eq. (4), to get a Stark broadening of only 0.1 nm with $T_e = 9000\ K$, an electron density of about $n_e \sim 3\ X\ 10^{15}\ cm^{-3}$ is required compared to that of the argon-hydrogen plasma of $n_e < 10^{10}\ cm^{-3}$ determined using a Langmuir probe, over five orders of magnitude less. Gigosos and Cardenoso [24] give the

observed Balmer $\alpha$ Stark broadening for plasmas of hydrogen with helium or argon as a function of the electron temperature and density. For example, the Stark broadening of the Balmer $\alpha$ line recorded on a $H + He^{+}$ plasma is only 0.033 nm with $T_e = 20{,}000\ K$ and $n_e = 1.4\ X\ 10^{14}\ cm^{-3}$. Thus, the Stark broadening was also insignificant. This result was also evident by the good fit to a Gaussian profile recorded on the argon-hydrogen plasma rather than a Voigt profile as shown in Figure 10.

A linear Stark effect arises from an applied electric field that splits the energy level with principal quantum number $n$ into $(2n-1)$ equidistant sublevels. The magnitude of this effect given by Videnovic et al. [8] is about $2\ X\ 10^{-2}\ nm/kV \cdot cm^{-1}$. No applied electric field was present in our study; thus, the linear Stark effect should be negligible.

To investigate whether the rt-plasmas of this study were optically thin or thick at a given frequency $\omega$, the effective path length $\tau_\omega(L)$ was calculated from

$$\tau_\omega(L) = \kappa_\omega L \tag{5}$$

where $L$ is the path length and $\kappa_\omega$ is the absorption coefficient given by

$$\kappa_\omega = \sigma_\omega\ X\ N_H \tag{6}$$

where $\sigma_\omega$ is the absorption cross section and $N_H$ is the number density of the absorber. For optically thin plasmas $\tau_\omega(L) < 1$, and for optically thick plasmas $\tau_\omega(L) > 1$. The absorption cross section for Balmer $\alpha$ emission is $\sigma = 8\ X\ 10^{-19}\ cm^2$ [30-32]. As discussed above, an estimate based on emission line profiles places the total H atom density of the argon-hydrogen plasma at $\sim 3.5\ X\ 10^{14}\ cm^{-3}$. Since this is overwhelmingly dominated by the ground state, $N_H = 3.5\ X\ 10^{14}\ cm^{-3}$ will be used. Thus, for a plasma length of $5\ cm$, $\tau_\omega(5\ cm)$ for Balmer $\alpha$ is

$$\tau_\omega(5\ cm) = \kappa_\omega L = \left(8\ X\ 10^{-19}\ cm^2\right)\left(3.5\ X\ 10^{14}\ cm^{-3}\right)(5\ cm) = 1.4\ X\ 10^{-3} \tag{7}$$

Since $\tau_\omega(5) <<< 1$, the argon-hydrogen plasmas were optically thin; so, the self absorption of 656.3 nm emission by n=1 state atomic hydrogen may be neglected as a source of the observed broadening.

Usually, the atomic hydrogen collisional cross section in plasmas is on the order of $10^{-18}\ cm^2$ [33]. Thus, for $N_H = 3.5\ X\ 10^{14}\ cm^{-3}$, collisional or pressure broadening is negligible.

A number of mechanisms have been proposed in order to explain the excessive Doppler broadening of the Balmer $\alpha$ line in argon-hydrogen

DC or RF driven glow discharge plasmas. Many of these have subsequently been shown to be untenable based on additional data or based on our results with microwave plasmas where no applied field is present. For example, Konjevic and Kuraica [7] observed $50\,eV$ anomalous thermal broadening of the Balmer lines during plane-cathode abnormal glow discharges of hydrogen-argon mixtures which was not observed with neon-hydrogen mixtures or pure hydrogen irrespective of cathode material, copper, carbon, or silver. To explain the excessive broadening with the presence of argon, they have proposed the quasiresonant charge-transfer process

$$Ar^{+(m)} + H_2 \rightarrow Ar + H_2^+ \tag{8}$$

with the further reaction

$$H_2^+ + H_2 \rightarrow H_3^+ + H \tag{9}$$

occurring to a significant extent due to its large cross section. The authors state:

> "However, in either case, it is essential that the $H_2^+$ or $H_3^+$ ion must gain energy in the electric field of the discharge before dissociation. Otherwise, the large energy of excited hydrogen atoms (on the average 50 eV per atom) cannot be explained."

In our experiments, the 110-130 eV line broadening observed in an argon-hydrogen microwave plasma can not be explained by this mechanism since no external field was present. In addition, broadening in argon-hydrogen plasmas can not be explained purely by a resonance energy transfer to $H_2^+$ which is accelerated in the electric field to dissociate as energetic atomic hydrogen as proposed by Kuraica and Konjevic [7]. Since the electric field is conservative, the symmetry of the broadened profile can not be explained simply by the acceleration of $H_2^+$ or any positive ion towards the cathode. This mechanism could only account for the red portion of the profile with the line of sight towards the cathode. A mechanism for the production of the blue portion that is symmetrical with the red portion is required. Such a mechanism was not suggested.

Djurovic and Roberts [22] recorded the spectral and spatial profiles of Balmer $\alpha$ line emission from low pressure RF (13.56 MHz) discharges

in $H_2 + Ar$ mixtures in a direction normal to the electric field. The introduction of Ar in a pure $H_2$ plasma increased the number of fast neutral atoms as evidenced by the intensity of the broad component of a two-component Doppler-broadened Balmer $\alpha$ line profile. Independent of cell position or direction, the average temperature of a wide profile component was 23.8 eV for voltages above 100 V, and the average temperature of a slow component was 0.22 eV. The mechanism proposed by Djurovic and Roberts is the production of fast H atoms from electric field accelerated $H_2^+$. The explanation of the role of Ar in the production of a large number of excited hydrogen atoms in the n=3 state, as well as raising their temperature for a given pressure and applied RF voltage, is that collisions with Ar in the plasma sheath region enhances the production of fast $H_2$ from accelerated $H_2^+$. The fast $H_2$ then undergoes dissociation to form fast H which may then be excited locally to the n=3 state by a further collision with Ar. The local excitation is a requirement since the atomic lifetime of the hydrogen n=3 state is approximately $10^{-8}\ s$, and the average velocity of the hydrogen atoms is $< 10^5$ m/s. Thus, the distance traveled must be less that 0.001 m.

The experimental evidence from several sources including ours does not support this mechanism. 1.) Only the number, but not the average energy (23.8 eV), of fast H-excited atoms was observed to be dependent of the position between the electrodes and the pressure for the same peak-to peak voltage (200 V). For a mechanism based on acceleration of any charged species in a special region such as the cathode fall region, this is unexpected. 2.) Since the measurements were taken perpendicular to the applied electric field, the symmetrical Doppler shape of both components centered at the same wavelength indicated that there were no directional velocity effects from the applied electric field. This would not be expected since the red and blue parts of the wings due to fast H must come from at least two different mechanisms. The red wing due to fast atoms moving toward the powered electrode arise from accelerated $H_2^+$; whereas, those moving away from the electrode arise from back scattered fast H atoms or fast H atoms formed on the electrode from decomposition of fast $H_2^+$ or fast $H_2$. Momentum transfer must occur at the electrode and gaps and/or asymmetries in the intensity would be expected for the proposed mechanism. A Maxwellian distribution would

not be anticipated from these different mechanisms; thus, a Gaussian line shape would not be anticipated. Rather a single source of fast H formed independent of direction is needed. 3.) Radovanov et al. [23] studied the excited neutrals and fast ions produced in a 13.56 MHz radio-frequency discharge in a 90% argon-10% hydrogen gas mixture by spatially and temporally resolved optical emission spectroscopy and by mass-resolved measurements of ion kinetic energy distributions at the grounded electrode. They concluded that a significant contribution of fast H atoms from $H_2^+$ is unlikely, due to the very fast conversion of $H_2^+$ to $H_3^+$. They determined that $H_3^+$ was the dominant light ion with $H^+$ and $H_2^+$ having intensities more than an order of magnitude. In addition, $H_3^+$ had the highest mean energy of the ions, even though $H^+$ exhibited the highest maximum kinetic energies. Based on these results, they concluded that $H_3^+$ rather than $H_2^+$ was the primary source of fast H emitted from the surface of the powered electrode. 4.) The Djurovic and Roberts mechanism of the excessive broadening caused by the addition of argon does not explain the lack of an effect with neon as shown by Kuraica and Konjevic [7]. Nor does it explain the lack of an effect with xenon or the greater effect with helium. 5.) All prior mechanisms to explain the excessive Balmer $\alpha$ line broadening in argon-hydrogen plasmas are based on the absolute requirement of an electric field which is absent in our microwave plasma experiments.

Videnovic et al. [8] explain the argon effect as due to the more efficient production of $H_3^+$. However, the most abundant ion in a pure hydrogen plasma is also $H_3^+$ [34]. And, according to Bogaerts and Gijbels [30] $H_3^+$ is the dominant hydrogen ion in argon-hydrogen plasmas due to the rapid reaction of $H_2^+$ with $H_2$. Videnovic et al. [8] claim the production of significant amounts of $H_3^+$ by participation of argon ion through reactions such as

$$Ar^+ + H_2 \rightarrow ArH^+ + H \qquad (10)$$

$$ArH^+ + H_2 \rightarrow H_3^+ + Ar \qquad (11)$$

However, Bogaerts and Gijbels [30] show that protonated argon is rapidly reduced by electrons. The reaction

$$ArH^+ + e^- \rightarrow Ar + H \qquad (12)$$

has a high rate constant of $k \sim 10^{-7}\ cm^3 s^{-1}$ [30]; whereas, the formation of $ArH^+$ is much slower. The rate constant and cross section for proton

transfer given by Eq. (10) are $k \sim 4\,X\,10^{-10} - 1.6\,X\,10^{-9}\ cm^3 s^{-1}$ and $\sigma \sim 2\,X\,10^{-15}\ cm^2$, respectively, [30] which are not favorable. Similarly, the rate constant and cross section for charge transfer given by

$$Ar^+ + H_2 \rightarrow Ar + H_2^+ \tag{13}$$

are $k \sim 2.7\,X\,10^{-10}$ and $\sigma \sim 10^{-15}\ cm^2$, respectively [30]. These reactions are very unlikely to contribute to the production of $H_3^+$ in an appreciable manner since the degree of ionization of argon is typically low, $10^{-5} - 10^{-4}$ [30]. And, $Ar$ actually contributes to the destruction of $H_3^+$ through the reaction

$$Ar + H_3^+ \rightarrow ArH^+ + H_2 \tag{14}$$

which has a significant cross section of $\sigma \sim 5\,X\,10^{-16}\ cm^2$

In addition, Videnovic et al. [8] propose the argon effect is due to the efficient production of $H_3^+$ via the production of $H_2^+$ by the reaction

$$Ar^+\left(3p^5\,^2P_0^{1/2}\right) + H_2 \rightarrow Ar + H_2^+ \tag{15}$$

The contribution by this pathway is also very unlikely to be significant due to the short lifetime of the excited state and corresponding negligible population.

Since hydrogen usually has a low degree of ionization, $10^{-4}$, and the cross section for electron ionization of molecular hydrogen:

$$e^- + H_2 \rightarrow e^- + e^- + H_2^+ \tag{16}$$

is $10^{-16}\ cm^2$, this reaction is expected to be the major source of $H_2^+$ even in argon-hydrogen plasmas [30]. The participation by argon should be insignificant when species concentrations, lifetimes, and reaction cross sections are considered. Furthermore, Videnovic et al. ignored other processes which could diminish the acceleration of hydrogen ions in the cathode fall region. For example, the dissociative recombination cross section for $H_3^+$ given by

$$e^- + H_3^+ \rightarrow H_2 + H \tag{17}$$

is $10^{-14}\ cm^2$ [30], about an order of magnitude greater than the cross section of Eq. (10) or Eq. (13) which may give rise to $H_3^+$. Thus, it is not apparent that $H_3^+$ could give rise to fast H even if it was produced in greater amounts with the addition of argon.

Videnovic et al. [8] propose that the absence of line broadening with argon alone is explained by a large cross section for charge-exchange which prevents the acceleration of argon ions to high energies. For example, the charge-exchange reaction

$$\left(Ar^{+}\right)_{f} + Ar_{s} \rightarrow Ar_{f} + \left(Ar^{+}\right)_{s} \qquad (18)$$

(s designates slow, and f designates fast) has a cross section of the order of $10^{-15}\ cm^{2}$, in the energy range 10-1000 eV. This cross section is about a factor of 30 times that for charge-exchange processes involving $H_3^+$ and $H^+$; thus, Videnovic et al. [8] argue that the diminished collisions result in higher energy ions reaching the cathode in the case of $H_3^+$ and $H^+$ compared to $Ar^+$. But, the cross section for $Ar^+$ is still very small corresponding to a mean free path at 30 mTorr pressure of about the width of the cathode fall region of 0.1-0.2 cm given by Videnovic et al. [8].

Similarly, their argument that argon gas is more transparent for back scattered fast H atoms than hydrogen gas is not persuasive. They calculate that 66% of reflected H atoms arrive at the negative glow region without collisions in the former case and 18% in the latter case at similar gas pressure and temperature ($T_g(Ar/H_2) = T_g(H_2) = 1000\ K$, $P(Ar/H_2) = 320\ Pa$, and $P(H_2) = 228\ Pa$). However, they assumed a cathode fall region that was twice the length in the hydrogen case ($L = 0.158\ cm$ versus $0.085\ cm$), and even if this factor of two difference existed, it could be compensated by reducing the hydrogen pressure to one half that of the argon-hydrogen plasma. In fact, intense excessive broadening is not observed in hydrogen with $P(H_2) = 150\ Pa$ [7]; whereas, it is in the case with $P(Ar/H_2) = 320\ Pa$.

Another argument against the greater transparency of argon is that although the intensity is much smaller, excessive broadening is observed at the cathode fall region for hydrogen alone which is greater (125 eV) than that observed in the case of an argon-hydrogen mixture (95 eV) [7].

A further internal inconsistency arises from the explanation of the argon effect by Radovanov et al. [23] compared to that of Videnovic et al. [8]. Radovanov et al. [23] conclude that in the sheath, the Doppler-shifted emission cannot be due primarily to electron collisions with fast H atoms, since calculations show that the electron density on the sheath region should be low. Rather, the emission from the fast H atoms stems from energetic ions or atoms formed near or at the powered electrode, and then are able to travel into the discharge volume before being collisionally excited to the n=3 state. The increase in Doppler-shifted

Balmer $\alpha$ emission when argon is added to $H_2$ is attributed to the high excitation cross section of fast H atoms. Thus, argon provides a collisionless environment according to Videnovic et al. [8] that allow ions to accelerate and fast H to propagate; yet, it is highly collisional according to Radovanov et al. [23] in order to form the excited n=3 atoms. This explanation is even less plausible given our observation with microwave plasmas that the largest broadening was observed with helium-hydrogen followed by argon-hydrogen, but no broadening was observed with neon or xenon with hydrogen.

Videnovic et al. [8] encounter another problem with the observation that the H temperature in the negative glow is higher than that in the cathode fall region. Their explanation is that fast neutrals are additionally excited by collisions with electrons. Yet, the electron temperature $T_e$ in these plasmas is only about 1 eV [7]; whereas, the H atom temperature $T_H$ in the negative glow region was about 50 eV. Since $T_H >>> T_e$ the energetic atoms would be expected to heat the electrons rather than the reverse process as proposed by Videnovic et al. [8].

Prior studies that reported high H temperatures attributed the observation to acceleration of ions in a high electric fields at the cathode fall region [7, 8, 22, 23] and an external field Stark effect [8]. We believe this is the first report of similar observations with a microwave plasma having no high field present. The microwave field couples to electrons, not ions. And, the high H temperature can not be attributed to the mechanisms proposed previously. In fact, the microwave case, the argon atoms and ions would have the highest energies since they have the largest cross section for electron collisions.

No hydrogen species, $H^+$, $H_2^+$, $H_3^+$, $H^-$, $H$, or $H_2$, responds to the microwave field; rather, only the electrons respond. But, the measured electron temperature was about 1 eV; whereas, the measured H temperature was 110-130 eV. This requires that $T_H >>> T_e$. This result can not be explained by electric field acceleration of charged species. In microwave driven plasmas, there is no high electric field in a cathode fall region ($> 1kV/cm$) to accelerate positive ions as proposed previously [7, 8, 22, 23] to explain significant broadening in hydrogen containing plasmas driven at a high voltage electrodes. It is impossible for $H$ or any $H$-containing ion which may give rise to $H$ to have a higher temperature

than the electrons in a microwave plasma. The observation of excessive Balmer line broadening in a microwave driven plasma requires a source of energy other than that provided by the electric field.

Excessive line broadening was observed in the case where $Ar^+$ was present with hydrogen, but not when xenon replaced argon. The distinction is that argon ion may form an rt-plasma. It provides a net positive enthalpy of reaction of $27.2\,eV$ (i.e. it resonantly accepts the nonradiative energy transfer from hydrogen atoms and releases the energy to the surroundings which heat up). The thermalization of the $27.2\,eV$ is consistent with the observation by Djurovic and Roberts [22] and Radovanov et al. [23] of no directional effects of the Doppler broadening due to the applied electric field and the average energy of 23.8 eV and 28 eV, receptively, of the fast H excited atoms that was similar throughput the whole interelectrode region of the discharge over a wide range of gas pressures, applied RF voltages, and hydrogen concentration in $Ar-H_2$ mixtures. In addition, at low pressures, Radovanov et al. [23] observed $Ar^+$ and $ArH^+$ kinetic energy distribution profiles with an edge at about $27.2\,eV$. Spectroscopy on these cell such as that given previously [35] and further studies with xenon could confirm the catalysis reaction.

Rt-plasmas formed with hydrogen-potassium mixtures have been reported previously [17-18] wherein the plasma decayed with a two second half-life when the electric field was set to zero. This was the thermal decay time of the filament which dissociated molecular hydrogen to atomic hydrogen. This experiment showed that hydrogen line emission was occurring even though the voltage between the heater wires was set to and measured to be zero and indicated that the emission was due to a reaction of potassium atoms with atomic hydrogen. Potassium atoms ionize at an integer multiple of the potential energy of atomic hydrogen, $m \cdot 27.2\,eV$. The enthalpy of ionization of $K$ to $K^{3+}$ has a net enthalpy of reaction of $81.7426\,eV$, which is equivalent to $m=3$. $K^{3+}$ and the formation of the corresponding hydride were detected by EUV spectroscopy recorded on an rt-plasma [12].

A rt-plasma of hydrogen and certain alkali ions formed at low temperatures (e.g. $\approx 10^3\,K$) as recorded via EUV spectroscopy, and an excessive afterglow duration was observed by hydrogen Balmer and

alkali line emissions in the visible range [18]. The observed plasma formed from atomic hydrogen generated at a tungsten filament that heated a titanium dissociator and one of potassium, rubidium, cesium, and their carbonates and nitrates. These atoms and ions ionize to provide a net enthalpy of reaction of an integer multiple of the potential energy of atomic hydrogen ($m \cdot 27.2\,eV$, $m = \text{integer}$) to within 0.17 eV and comprise only a single ionization in the case of a potassium or rubidium ion. Whereas, the chemically similar atoms of sodium and sodium and lithium carbonates and nitrates which do not ionize with these constraints caused no emission. To test the electric dependence of the emission, the weak electric field of about 1 V/cm was set and measured to be zero in $< 0.5\,X\,10^{-6}$ sec. An afterglow duration of about one to two seconds was recorded in the case of potassium, rubidium, cesium, $K_2CO_3$, $RbNO_3$, and $CsNO_3$. Hydrogen line or alkali line emission was occurring even though the voltage between the heater wires was set to and measured to be zero. These atoms and ions ionize to provide a net enthalpy of reaction of an integer multiple of the potential energy of atomic hydrogen to within less than the thermal energies at $\approx 10^3\,K$ and comprise only a single ionization in the case of a potassium or rubidium ion. Since the thermal decay time of the filament for dissociation of molecular hydrogen to atomic hydrogen was similar to the rt-plasma afterglow duration, the emission was determined to be due to a reaction of atomic hydrogen with each of the atoms or ions that did not require the presence of an electric field to be functional.

### C. Balmer $\alpha$ line broadening recorded on capacitively coupled RF discharge plasmas

The 656.3 nm Balmer $\alpha$ line width recorded normal to the applied electric field direction with a high resolution ($\pm 0.006\,nm$) visible spectrometer on capacitively coupled RF discharge plasmas discharge plasmas of hydrogen compared with each of xenon-hydrogen (90/10%) and argon-hydrogen (90/10%) are shown in Figures 11 and 12, respectively. To illustrate the method of displaying each line broadening result as an unsmoothed curve, the corresponding raw data points are also shown that further show the scatter in the data. The energetic

hydrogen atom densities and energies of the plasmas of hydrogen alone and hydrogen-noble gas mixtures were calculated using the method of Videnovic et al. [8] and are given in Table 3. In the capacitively coupled RF cells, the Balmer $\alpha$ line profile comprised two distinct Gaussian peaks, an inner, narrower peak corresponding to a slow component with an average hydrogen energy of 3-4 eV in addition to an outer broader peak corresponding to a fast component as reported in Table 4. This slow population is assigned to thermal excitation in the plasma and matches those reported previously [22]. It was found that the helium-hydrogen and argon-hydrogen capacitively coupled RF plasmas showed extraordinary broadening corresponding to an average hydrogen atom temperature of $30-40\,eV$ and $50-60\,eV$, respectively, and an atom density of $1.1\,X\,10^{14} \pm 20\%\ atoms/cm^3$ and $1.8\,X\,10^{14} \pm 20\%\ atoms/cm^3$, respectively. Whereas, pure hydrogen, neon-hydrogen, and xenon-hydrogen showed no excessive broadening corresponding to an average hydrogen atom temperature of $\leq 3\,eV$. The maximum atom density of only $5.5\,X\,10^{13} \pm 20\%\ atoms/cm^3$ was observed with pure hydrogen as the test gas even though 10 times more hydrogen was present.

The broadening was not dependent on the input power over the range studied. No voltage effect was observed; even though, the corresponding voltage range was over 100 V [22-23]. Thus, high electric fields can not explain the observed line broadening. This point was confirmed by the absence of broadening with hydrogen alone.

### D. Balmer $\alpha$ line broadening and $T_e$ measurements recorded on inductively coupled RF discharge plasmas

The 656.3 nm Balmer $\alpha$ line width recorded with a high resolution ($\pm 0.006\,nm$) visible spectrometer on inductively coupled RF discharge plasmas of hydrogen compared with each of xenon-hydrogen (90/10%) and argon-hydrogen (90/10%) are shown in Figures 13 and 14, respectively. The helium-hydrogen (90/10%) Balmer $\alpha$ line width profile is compared to that of argon-hydrogen (90/10%) in Figure 15. The energetic hydrogen atom densities and energies of plasmas of hydrogen alone and noble gas-hydrogen mixtures were calculated using the method of Videnovic et al. [8] and are given in Table 5. It was found that the

inductively coupled RF helium-hydrogen and argon-hydrogen plasmas showed extraordinary broadening corresponding to an average fast hydrogen atom temperature of $250-310\,eV$ and $180-230\,eV$, respectively, and an atom density of $7.5\,X\,10^{14}\pm 20\%\,atoms/cm^3$ and $4.6\,X\,10^{14}\pm 20\%\,atoms/cm^3$, respectively. Whereas, pure hydrogen, neon-hydrogen, and xenon-hydrogen showed no excessive broadening corresponding to an average hydrogen atom temperature of $\approx 4\,eV$. The maximum atom density of only $9\,X\,10^{13}\pm 20\%\,atoms/cm^3$ was observed with pure hydrogen as the test gas even though 10 times more hydrogen was present.

The hydrogen plasma emission was statistically well fit by a single Gaussian curve as shown in Figure 16. Whereas, the argon-hydrogen plasma emission matched two Gaussian profiles as shown in Figure 17. Significant broadening was observed for both curves corresponding to slow and fast hydrogen atoms having an average hydrogen atom temperature of $30-35\,eV$ and $180-230\,eV$, respectively, as shown in Table 4.

These studies demonstrate excessive line broadening in the absence of an observable effect attributable to a strong electric field since the hydrogen emission shows no broadening. No power or voltage dependence of the broadening was observed over the range studied, 40-100 W and RF voltages of about 40 V [36].

A comparison of the different light sources for helium hydrogen and argon-hydrogen plasmas is given in Table 4. The broadening in helium hydrogen plasmas was greater than that in argon-hydrogen plasmas for all light sources except in the case of the capacitively coupled RF discharge. The inductively coupled RF plasma source had the greatest line broadening of any source followed by the microwave plasma source which was vastly greater than the capacitively coupled RF and discharge plasma sources. If the electric field was the source of the broadening, then the discharge cell would be anticipated to show the greatest broadening since the electric field in the cathode fall region was at least $1\,kV/cm$. Whereas, essentially no broadening would be expected from the microwave or inductively coupled RF plasmas since no field and one that was one to two orders of magnitude weaker were present, respectively. The broadening observations were counter to the electric field

relationship.

The results of the Langmuir probe measurements for the electron density $n_e$ for the capacitively coupled RF, discharge, inductively coupled RF, and microwave plasma cells were $10^{10}$-$10^{11}$ $cm^{-3}$ [22-23], $10^{9}$-$10^{11}$ $cm^{-3}$ [7], $10^{9}$ $cm^{-3}$ [36], and $<10^{9}$ $cm^{-3}$ (measured), respectively. The electron density measurements by Langmuir probe shows that the trend in electron density was capacitively coupled RF = discharge > inductively coupled RF cell > microwave. Whereas, the trend in broadening of the Balmer $\alpha$ line was the opposite. No power or voltage dependence of the broadening was observed for any of the plasma sources studied. Neither the electron Stark effect nor any of the other conventional broadening mechanisms discussed in Sec. IIIB can explain these results.

The results of the $T_e$ measurements on inductively coupled RF discharge plasmas of pure hydrogen alone and a mixture of 10% hydrogen and helium, neon, argon, or xenon are given in Table 5. Similarly to the ion measurement, the average electron temperatures of helium-hydrogen and argon-hydrogen plasmas were high, $39{,}600 \pm 5\%\ K$ and $15{,}800 \pm 5\%\ K$, respectively. Whereas, the corresponding temperatures of xenon-hydrogen and hydrogen alone plasmas were only $7590 \pm 5\%\ K$, and $6000 \pm 5\%\ K$, respectively.

In this case of the inductively coupled RF discharge as well as the those of the capacitively coupled RF discharge, microwave, and discharge light sources, excessive line broadening and an elevated electron temperature was only observed in the cases where an ion was present which could provide a net enthalpy of reaction of an integer multiple of the potential energy of atomic hydrogen ($Ar^+$ or $He^+$). Whereas plasmas of chemically similar controls that do not provide gaseous atoms or ions that have electron ionization energies which are close match to a multiple of $27.2\ eV$ showed no broadening or elevated $T_e$ compared to pure hydrogen. These support the rt-plasma mechanism.

## IV. SUMMARY AND CONCLUSIONS

Line broadening of the hydrogen Balmer lines provides a sensitive measure of the number and energy of excited hydrogen atoms in a glow discharge plasma. The width of the 656.3 nm Balmer $\alpha$ line emitted

from glow discharge plasmas having atomized hydrogen from pure hydrogen alone and a mixture of 10% hydrogen and helium, argon, neon, or xenon was measured with a high resolution ($\pm 0.025\ nm$) visible spectrometer. The energetic hydrogen atom density and energies were determined from the broadening, and it was found that helium-hydrogen and argon-hydrogen showed significant broadening corresponding to an average hydrogen atom temperature of $30-38\ eV$ and an atom density of $3\ X\ 10^{13} \pm 20\%\ atoms/cm^3$; whereas, pure hydrogen, neon-hydrogen, and xenon-hydrogen showed no excessive broadening corresponding to an average hydrogen atom temperature of $\approx 4\ eV$. The maximum atom density of only $5\ X\ 10^{13} \pm 20\%\ atoms/cm^3$ was observed with pure hydrogen as the test gas even though 10 times more hydrogen was present. Thus, line broadening and high atom densities were only observed for the ions which provided a net enthalpy of reaction of a multiple of the potential energy of the hydrogen atom ($Ar^+$ or $He^+$).

Kuraica and Konjevic [7] and Videnovic et al. [8] studied 97% argon and 3% hydrogen mixtures in Grimm-type discharges with a hollow anode. In our studies with argon-hydrogen plasmas, the voltage was increased at 50 V increments from 275 V to 475 V, and the high resolution visible spectra were recorded to observe the effect of voltage on the Balmer $\alpha$ line broadening. In contrast to an increase in broadening with voltage predicted by Kuraica and Konjevic [7], no voltage effect was observed in our normal discharge studies which supports the rt-plasma mechanism as the source of the excessive broadening.

The 656.3 nm Balmer $\alpha$ line width measurements were repeated with microwave and inductively and capacitively coupled RF discharge plasmas rather than the glow discharge plasmas, and significant differences were observed between the plasma source while the same trend was observed for the particular plasma gas. It was found that inductively coupled RF helium-hydrogen and argon-hydrogen plasmas showed extraordinary broadening corresponding to an average hydrogen atom temperature of $250-310\ eV$ and $180-230\ eV$, respectively, and an atom density of $4.8\ X\ 10^{14} \pm 20\%\ atoms/cm^3$ and $3.5\ X\ 10^{14} \pm 20\%\ atoms/cm^3$, respectively, compared to an average hydrogen atom temperature of $30-40\ eV$ and $50-60\ eV$, respectively, and an atom density of $1.1\ X\ 10^{14} \pm 20\%\ atoms/cm^3$ and $1.8\ X\ 10^{14} \pm 20\%\ atoms/cm^3$, respectively, for the

corresponding capacitively coupled plasmas. A slow as well as a fast population of H atoms was observed for both types of RF cells with helium-hydrogen and argon-hydrogen plasmas. However, the slow population was about an order of magnitude more energetic in the case of the inductively coupled plasma cell—$\approx 3\,eV$ versus $\approx 30\,eV$.

Microwave helium-hydrogen and argon-hydrogen plasmas showed significant broadening corresponding to an average hydrogen atom temperature of $180\text{-}210\,eV$ and $110\text{-}130\,eV$, respectively, and an atom density of $4.8\,X\,10^{14} \pm 20\%\ atoms/cm^3$ and $3.5\,X\,10^{14} \pm 20\%\ atoms/cm^3$, respectively. In contrast, similar to the results of the discharge cell, the corresponding average atom temperature of $\approx 1-4\,eV$ was observed for plasmas of pure hydrogen, neon-hydrogen, and xenon-hydrogen maintained in any of the microwave and inductively and capacitively coupled RF discharge plasma sources. For inductively and capacitively coupled RF and microwave discharge plasmas, the maximum atom density of only $9\,X\,10^{13} \pm 20\%\ atoms/cm^3$, $5.5\,X\,10^{13} \pm 20\%\ atoms/cm^3$, and $7\,X\,10^{13} \pm 20\%\ atoms/cm^3$, respectively, was observed with pure hydrogen as the test gas even though 10 times more hydrogen was present.

Similarly, the average electron temperature $T_e$ for helium-hydrogen and argon-hydrogen inductively coupled RF and microwave plasmas were high, $39{,}600 \pm 5\%\,K$, $15{,}800 \pm 5\%\,K$, $28{,}000 \pm 5\%\,K$, and $11{,}600 \pm 5\%\,K$, respectively; compared to $7590 \pm 5\%\,K$, $6000 \pm 5\%\,K$, $6500 \pm 5\%\,K$, and $5500 \pm 5\%\,K$ for the corresponding plasmas of xenon-hydrogen and hydrogen alone, respectively.

Excessive line broadening and an elevated electron temperature were only observed for the ions which provided a net enthalpy of reaction of a multiple of the potential energy of the hydrogen atom. The electron density was far too low for detectable Stark broadening, and the trend in $n_e$ was opposite that of the broadening. And, no electric field was present in the microwave plasmas. Thus, the results can not be explained by external Stark broadening or acceleration of charged species due to high fields of over $10\,kV/cm$ as proposed by Videnovic et al. [8] to explain excessive broadening observed in glow discharges. Similarly, previous explanations based on field acceleration of ions at the powered electrode of RF cells are insufficient [22-23]. The results are consistent with an energetic reaction caused by a resonance energy transfer

between hydrogen atoms and $Ar^+$ or $He^+$ as the source of the excessive line broadening. The reaction rate was higher under the conditions of a inductively coupled RF or microwave compared to a capacitively coupled RF or glow discharge plasma even at a lower input power.

## ACKNOWLEDGMENT

Special thanks to Fred Becker for technical support with the RF plasma systems and to O. Klueva of Jobin Yvon Horiba, Inc, Edison, NJ for assistance and use of the high resolution ($\pm 0.025\,nm$) visible spectrometer.

## REFERENCES

1. P. W. J. M. Boumans, Spectrochim. Acta Part B, 46 (1991) 711.
2. J. A. C. Broekaert, Appl. Spectrosc., 49, (1995) 12A.
3. P. W. J. M. Boumans, J. A. C. Broekaert, and R. K. Marcus, Eds., Spectrochim. Acta Part B, 46 (1991) 457.
4. M. Dogan, K. Laqua, and H. Massmann, "Spektrochemische Analysen mit einer Glimmentladungslampe als Lichtquelle—I," Spectrochim. Acta, Volume 26B, (1971) 631–649.
5. M. Dogan, K. Laqua, and H. Massmann, "Spektrochemische Analysen mit einer Glimmentladungslampe als Lichtquelle—II, "Spectrochim. Acta, Volume 27B, (1972) 65–88.
6. J. A. C. Broekaert, J. Anal. At. Spectrom., 2 (1987) 537.
7. M. Kuraica, N. Konjevic, "Line shapes of atomic hydrogen in a plane-cathode abnormal glow discharge", Physical Review A, Volume 46, No. 7, October (1992), pp. 4429-4432.
8. I. R. Videnovic, N. Konjevic, M. M. Kuraica, "Spectroscopic investigations of a cathode fall region of the Grimm-type glow discharge", Spectrochimica Acta, Part B, Vol. 51, (1996), pp. 1707-1731.
9. P. Kurunczi, H. Shah, and K. Becker, "Hydrogen Lyman-$\alpha$ and Lyman-$\beta$ emissions from high-pressure microhollow cathode discharges in $Ne-H_2$ mixtures", J. Phys. B: At. Mol. Opt. Phys., Vol. 32, (1999), L651-L658.
10. M. Parker and R. K. Marcus, Appl. Spectrosc., 48, (1994) 623.
11. J. A. R. Sampson, *Techniques of Vacuum Ultraviolet Spectroscopy*, Pied

Publications, (1980), pp. 94-179.
12. R. Mills, P. Ray, "Spectroscopic Identification of a Novel Catalytic Reaction of Potassium and Atomic Hydrogen and the Hydride Ion Product", Int. J. Hydrogen Energy, Vol. 27, No. 2, February, (2002), pp. 183-192.
13. R. Mills, "Spectroscopic Identification of a Novel Catalytic Reaction of Atomic Hydrogen and the Hydride Ion Product", Int. J. Hydrogen Energy, Vol. 26, No. 10, (2001), pp. 1041-1058.
14. R. Mills and M. Nansteel, "Argon-Hydrogen-Strontium Discharge Light Source", IEEE Transactions on Plasma Science, in press.
15. R. Mills, M. Nansteel, and Y. Lu, "Excessively Bright Hydrogen-Strontium Plasma Light Source Due to Energy Resonance of Strontium with Hydrogen", Plasma Chemistry and Plasma Processing, submitted.
16. R. Mills, J. Dong, Y. Lu, "Observation of Extreme Ultraviolet Hydrogen Emission from Incandescently Heated Hydrogen Gas with Certain Catalysts", Int. J. Hydrogen Energy, Vol. 25, (2000), pp. 919-943.
17. R. Mills, "Temporal Behavior of Light-Emission in the Visible Spectral Range from a Ti-K2CO3-H-Cell", Int. J. Hydrogen Energy, Vol. 26, No. 4, (2001), pp. 327-332.
18. R. Mills, T. Onuma, and Y. Lu, "Formation of a Hydrogen Plasma from an Incandescently Heated Hydrogen-Catalyst Gas Mixture with an Anomalous Afterglow Duration", Int. J. Hydrogen Energy, Vol. 26, No. 7, July, (2001), pp. 749-762.
19. R. Mills, M. Nansteel, and Y. Lu, "Observation of Extreme Ultraviolet Hydrogen Emission from Incandescently Heated Hydrogen Gas with Strontium that Produced an Anomalous Optically Measured Power Balance", Int. J. Hydrogen Energy, Vol. 26, No. 4, (2001), pp. 309-326.
20. R. Mills, P. Ray, "Spectral Emission of Fractional Quantum Energy Levels of Atomic Hydrogen from a Helium-Hydrogen Plasma and the Implications for Dark Matter", Int. J. Hydrogen Energy, Vol. 27, No. 3, pp. 301-322.
21. S. Alexiou, E. Leboucher-Dalimier, "Hydrogen Balmer-$\alpha$ in dense plasmas", Phys, Rev. E, Vol. 60, No. 3, (1999), pp. 3436-3438.
22. S. Djurovic, J. R. Roberts, "Hydrogen Balmer alpha line shapes for hydrogen -argon mixtures in a low-pressure rf discharge", J. Appl. Phys., Vol. 74, No. 11, (1993), pp. 6558-6565.

23. S. B. Radovanov, K. Dzierzega, J. R. Roberts, J. K. Olthoff, Time-resolved Balmer-alpha emission from fast hydrogen atoms in low pressure, radio-frequency discharges in hydrogen", Appl. Phys. Lett., Vol. 66, No. 20, (1995), pp. 2637-2639.
24. M. A. Gigosos, V. Cardenoso, "New plasma diagnosis tables of hydrogen Stark broadening including ion dynamics", J. Phys. B: At. Mol. Opt. Phys., Vol. 29, (1996), pp. 4795-4838.
25. NIST Atomic Spectra Database, www.physics.nist.gov/cgi-bin/AtData/display.ksh.
26. H. R. Griem, *Principle of Plasma Spectroscopy*, Cambridge University Press, (1987).
27. R. Mayo, R. Mills, M. Nansteel, "Direct Plasmadynamic Conversion of Plasma Thermal Power to Electricity", IEEE Transactions on Plasma Science, submitted.
28. J. Seidel, "Theory of two-photon polarization spectroscopy of plasma-broadened hydrogen $L_\alpha$ line", Phys. Rev. Letts., Vol. 57, No. 17, (1986), p. 2154.
29. A. Czernikpwski, J. Chapelle, Acta Phys. Pol. A., Vol. 63, (1983), p. 67.
30. A. Bogaerts, R. Gijbels, "Effects of adding hydrogen to an argon glow discharge: overview of some relevant processes and some quantitative explanations", Journal of Analytical Atomic Spectroscopy, Vol. 15, (2000), pp. 441-449.
31. J. M. Ajello, D. Shemansky, T. L. Kwok, Y. L. Yung, "Studies of extreme-ultraviolet emission from Rydberg series of $H_2$ by electron impact", Physical Review A, Vol. 29, No. 2, (1984), p. 636.
32. J. M. Ajello, S. K. Srivastava, Y. L. Yung, "Laboratory studies of UV emissions of $H_2$ by electron impact. The Werner- and Lyman-band systems", Physical Review A, Vol. 25, No. 5, (1982), p. 2485
33. A. Corney, Atomic and Laser Spectroscopy, Clarendon Press, Oxford, (1977).
34. C. Chen, T. Wei, L. R. Collins, and J. Phillips, "Modeling the discharge region of a microwave generated hydrogen plasma", J. Phys. D: Appl. Phys., Vol. 32, (1999), pp. 688-698.
35. R. Mills, P. Ray, "Vibrational Spectral Emission of Fractional-Principal-Quantum-Energy-Level Hydrogen Molecular Ion", Int. J. Hydrogen Energy, Vol. 27, No. 5, (2002), pp. 533-564.

36. D. Barton, J. W. Bradley, D. A. Steele, and R. D. Short, "investigating radio frequency plasmas used for the modification of polymer surfaces," J. Phys. Chem. B, Vol. 103, (1999), pp. 4423-4430.

Table 1. The energetic hydrogen atom densities and energies for catalyst and noncatalyst glow discharge plasmas.

| Plasma Gas | Hydrogen Atom Density[a] ($10^{13}$ $atoms/cm^3$) (±20%) | Hydrogen Atom Energy[b] ($eV$) (±5%) |
|---|---|---|
| $H_2$ | 5 | 3-4 |
| $Ne/H_2$ | 2.1 | 5-6 |
| $Xe/H_2$ | 1 | 3-4 |
| $Ar/H_2$ | 3 | 30-35 |
| $He/H_2$ | 3 | 33-38 |

[a] Approximate calculated after [8]

[b] Calculated after [8]

Table 2. The energetic hydrogen atom densities and energies and the electron temperature for catalyst and noncatalyst microwave discharge plasmas.

| Plasma Gas | Hydrogen Atom Density[a] ($10^{13}$ $atoms/cm^3$) (±20%) | Fast Hydrogen Atom Energy[b] ($eV$) (±5%) | Electron Temperature $T_e$[c] (K) (±5%) |
|---|---|---|---|
| $H_2$ | 7 | 3-5 | 5500 |
| $Ne/H_2$ | 9 | 5-6 | 7800 |
| $Xe/H_2$ | 3 | 3-4 | 6500 |
| $Ar/H_2$ | 35 | 110-130 | 11,600 |
| $He/H_2$ | 48 | 180-210 | 28,000 |

[a] Approximate calculated after [8]

[b] Calculated after [8]

[c] Calculated after [26]

Table 3. The energetic hydrogen atom densities and energies for catalyst and noncatalyst capacitively coupled RF plasmas.

| Plasma Gas | Hydrogen Atom Density[a] ($10^{13}$ *atoms*/*cm*$^3$) (±20%) | Hydrogen Atom Energy[b] (*eV*) (±5%) |
|---|---|---|
| $H_2$ | 5.5 | 1-2 |
| $Ne/H_2$ | 4.6 | 2-3 |
| $Xe/H_2$ | 1.8 | 2-3 |
| $Ar/H_2$ | 18 | 50-60 |
| $He/H_2$ | 11 | 30-40 |

[a] Approximate calculated after [8]

[b] Calculated after [8]

[c] Calculated after [26]

Table 4. The comparison of the energies of the slow and fast atoms of argon-hydrogen and helium-hydrogen glow discharge, microwave, capacitively coupled RF, and inductively coupled RF plasmas.

| Plasma System | Hydrogen Atom Energy[a] ($eV$) ($\pm 5\%$) | | | | |
|---|---|---|---|---|---|
| | Pure $H_2$ | $Ar/H_2$ | | $He/H_2$ | |
| | | Slow | Fast | Slow | Fast |
| Glow Discharge | 3-4 | | 30-35 | | 35-40 |
| Microwave Discharge | 3-5 | | 100-130 | | 180-210 |
| Capacitively Coupled RF | 1-2 | 3-5 | 50-60 | 3-5 | 30-40 |
| Inductively Coupled RF | 3-5 | 30-35 | 180-230 | 35-40 | 250-310 |

[a] Calculated after [8]

Table 5. The energetic hydrogen atom densities and energies and the electron temperature for catalyst and noncatalyst inductively coupled RF discharge plasmas.

| Plasma Gas | Hydrogen Atom Density[a] ($10^{13}$ $atoms/cm^3$) (±20%) | Fast Hydrogen Atom Energy[b] ($eV$) (±5%) | Electron Temperature $T_e$[c] (K) (±5%) |
|---|---|---|---|
| $H_2$ | 9 | 3-5 | 6000 |
| $Ne/H_2$ | 17 | 6-8 | 13,600 |
| $Xe/H_2$ | 3.6 | 3-5 | 7590 |
| $Ar/H_2$ | 46 | 180-230 | 15,800 |
| $He/H_2$ | 75 | 250-310 | 39,600 |

[a] Approximate calculated after [8]

[b] Calculated after [8]

[c] Calculated after [26]

Figure Captions

Figure 1. Cylindrical stainless steel cell for studies of the broadening of the Balmer $\alpha$ line emitted from glow discharge plasmas of 1.) pure hydrogen alone and 2.) a mixture of 10% hydrogen and helium, argon, neon, or xenon.

Figure 2. The experimental set up comprising a microwave discharge cell light source and an EUV spectrometer which was differentially pumped.

Figure 3. The experimental set up comprising a capacitively coupled RF cell light source.

Figure 4. The experimental set up comprising a inductively coupled RF cell light source and an EUV spectrometer which was differentially pumped.

Figure 5. The 656.3 nm Balmer $\alpha$ line width recorded with a high resolution ($\pm 0.025\,nm$) visible spectrometer on a xenon-hydrogen (90/10%) and a hydrogen glow discharge plasma. No line excessive broadening was observed corresponding to an average hydrogen atom temperature of $3-4\,eV$.

Figure 6. The 656.3 nm Balmer $\alpha$ line width recorded with a high resolution ($\pm 0.025\,nm$) visible spectrometer on an helium-hydrogen (90/10%) and a hydrogen glow discharge plasma. Significant broadening was observed corresponding to an average hydrogen atom temperature of $33-38\,eV$.

Figure 7. The 656.3 nm Balmer $\alpha$ line width recorded with a high resolution ($\pm 0.006\,nm$) visible spectrometer on a xenon-hydrogen (90/10%) and a hydrogen microwave discharge plasma. No line excessive broadening was observed corresponding to an average hydrogen atom temperature of $3-5\,eV$.

Figure 8. The 656.3 nm Balmer $\alpha$ line width recorded with a high resolution ($\pm 0.006\,nm$) visible spectrometer on a helium-hydrogen (90/10%) and a hydrogen microwave discharge plasma. Significant broadening was observed corresponding to an average hydrogen atom temperature of $180-210\,eV$.

Figure 9. The statistical curve fit of the Balmer $\alpha$ line width profile recorded on a hydrogen microwave plasma. The data matched a Gaussian

profile having the $X^2$ and R values of 0.00092 and 0.98937, respectively. No line excessive broadening was observed corresponding to an average hydrogen atom temperature of $3-5\,eV$.

Figure 10. The statistical curve fit of the Balmer $\alpha$ line width profile recorded on an argon-hydrogen microwave plasma. The data matched a Gaussian profile having the $X^2$ and R values of 0.00027 and 0.99192, respectively. Significant broadening was observed corresponding to an average hydrogen atom temperature of $110\text{-}130\,eV$.

Figure 11. The 656.3 nm Balmer $\alpha$ line width recorded with a high resolution ($\pm 0.006\,nm$) visible spectrometer on a xenon-hydrogen (90/10%) and a hydrogen capacitively coupled RF plasma. To illustrate the method of displaying each line broadening result as an unsmoothed curve, the corresponding raw data points are also shown that further show the scatter in the data. No line excessive broadening was observed corresponding to an average hydrogen atom temperature of $2-3\,eV$.

Figure 12. The 656.3 nm Balmer $\alpha$ line width recorded with a high resolution ($\pm 0.006\,nm$) visible spectrometer on argon-hydrogen (90/10%) and a hydrogen capacitively coupled RF plasma. Significant broadening was observed corresponding to an average hydrogen atom temperature of $50\text{-}60\,eV$.

Figure 13. The 656.3 nm Balmer $\alpha$ line width recorded with a high resolution ($\pm 0.006\,nm$) visible spectrometer on a xenon-hydrogen (90/10%) and a hydrogen inductively coupled RF plasma. No line excessive broadening was observed corresponding to an average hydrogen atom temperature of $3-5\,eV$.

Figure 14. The 656.3 nm Balmer $\alpha$ line width recorded with a high resolution ($\pm 0.006\,nm$) visible spectrometer on an argon-hydrogen (90/10%) and a hydrogen inductively coupled RF plasma. Significant broadening was observed corresponding to an average hydrogen atom temperature of $180-230\,eV$..

Figure 15. The 656.3 nm Balmer $\alpha$ line width recorded with a high resolution ($\pm 0.006\,nm$) visible spectrometer on helium-hydrogen (90/10%), and argon-hydrogen (90/10%) inductively coupled RF plasma. Significant broadening was observed for helium-hydrogen and argon-hydrogen corresponding to an average hydrogen atom temperature of $250-310\,eV$ and $180-230\,eV$, respectively.

Figure 16. The statistical curve fit of the Balmer $\alpha$ line width profile recorded on a hydrogen inductively coupled RF plasma The data matched a Gaussian profile having the $X^2$ and R values of 0.00434 and 0.98895, respectively. No line excessive broadening was observed corresponding to an average hydrogen atom temperature of $3-5\,eV$.

Figure 17. The statistical curve fit of the Balmer $\alpha$ line width profile recorded on an argon-hydrogen (90/10%) inductively coupled RF plasma. The data matched two Gaussian profiles having the $X^2$ and R values of 0.01039 and 0.99255, respectively. Significant broadening was observed for both curves corresponding to slow and fast hydrogen atoms having an average hydrogen atom temperature of $30-35\,eV$ and $180-230\,eV$, respectively, as shown in Table 4.

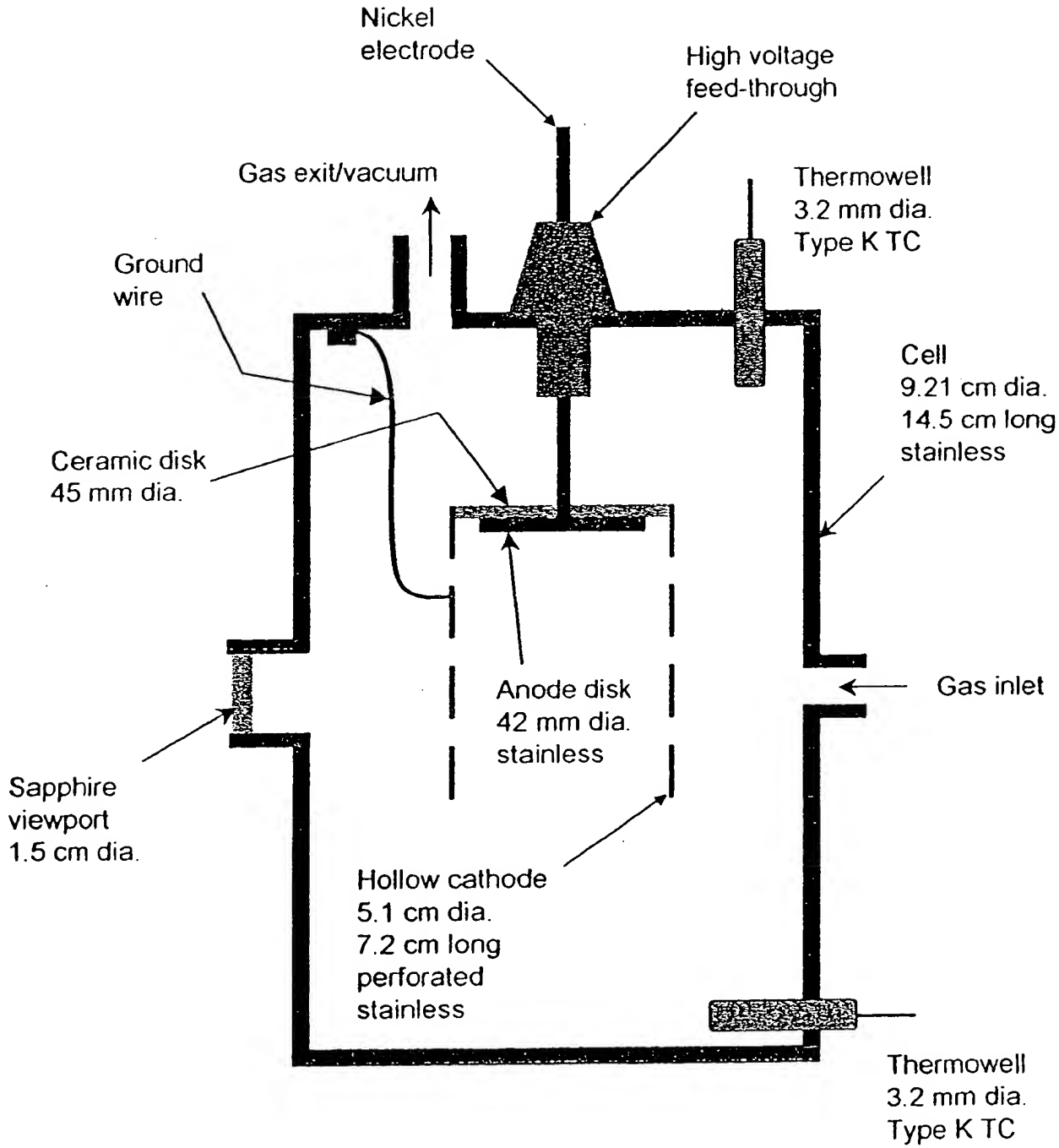
Nickel electrode
High voltage feed-through
Gas exit/vacuum
Thermowell 3.2 mm dia. Type K TC
Ground wire
Cell 9.21 cm dia. 14.5 cm long stainless
Ceramic disk 45 mm dia.
Anode disk 42 mm dia. stainless
Gas inlet
Sapphire viewport 1.5 cm dia.
Hollow cathode 5.1 cm dia. 7.2 cm long perforated stainless
Thermowell 3.2 mm dia. Type K TC

Fig. 1

Fig. 1

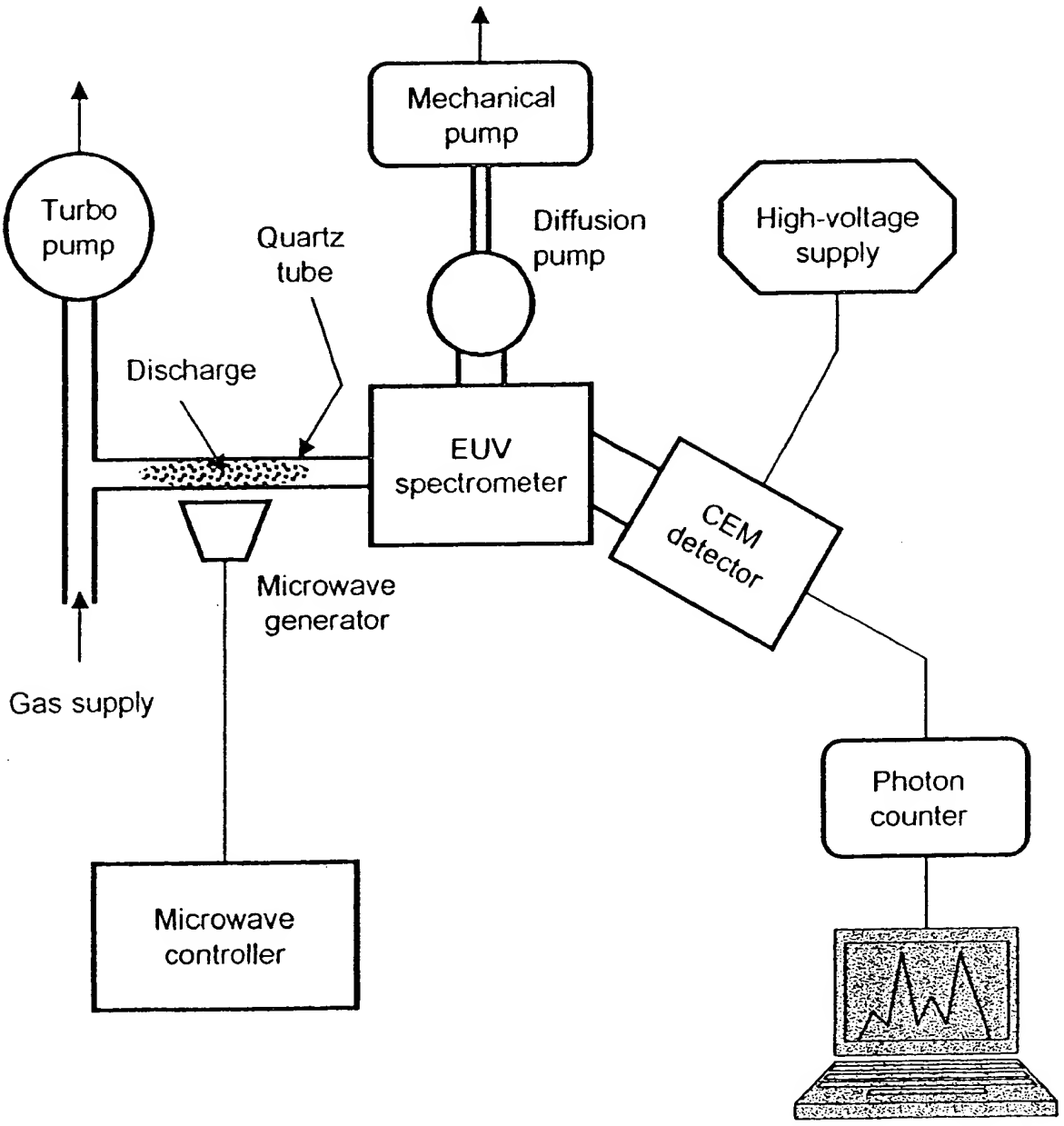
Mechanical pump
Turbo pump
Quartz tube
Diffusion pump
High-voltage supply
Discharge
EUV spectrometer
CEM detector
Microwave generator
Gas supply
Photon counter
Microwave controller

Fig. 2

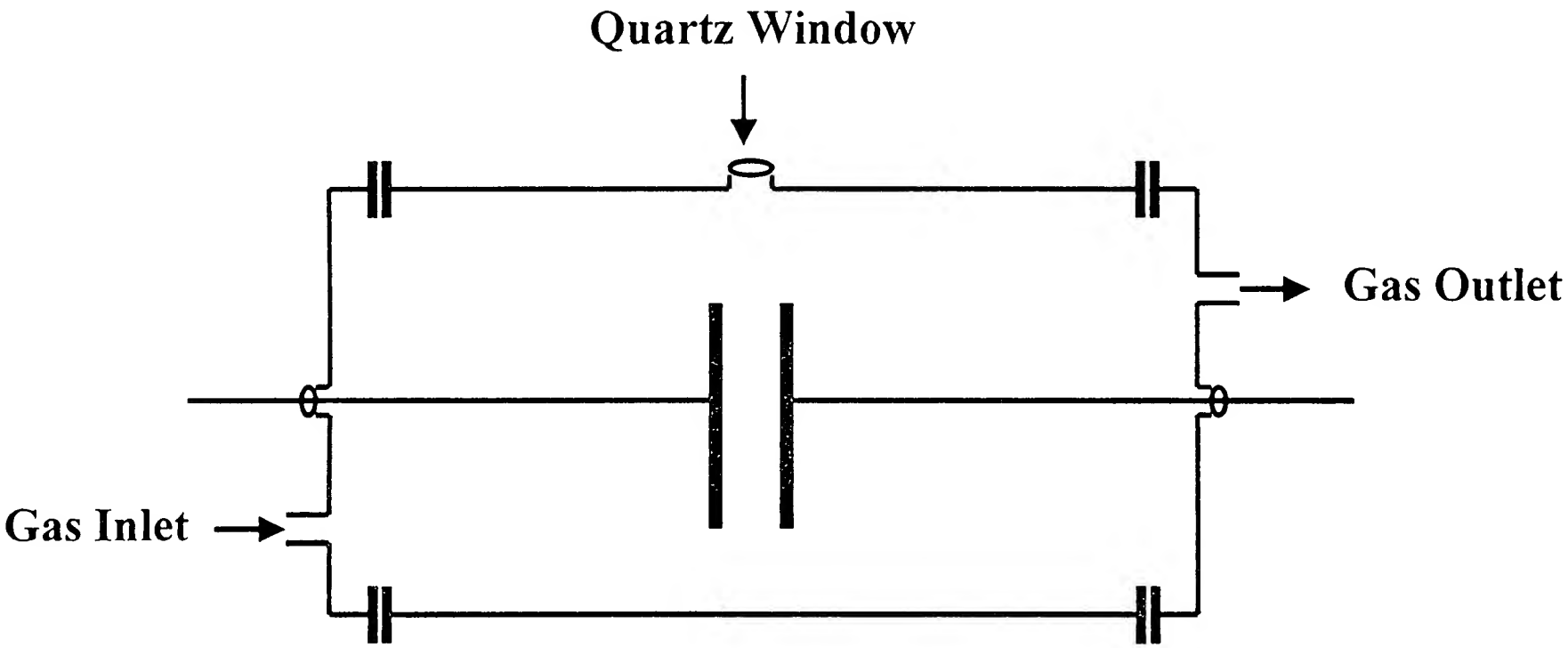


Fig. 3

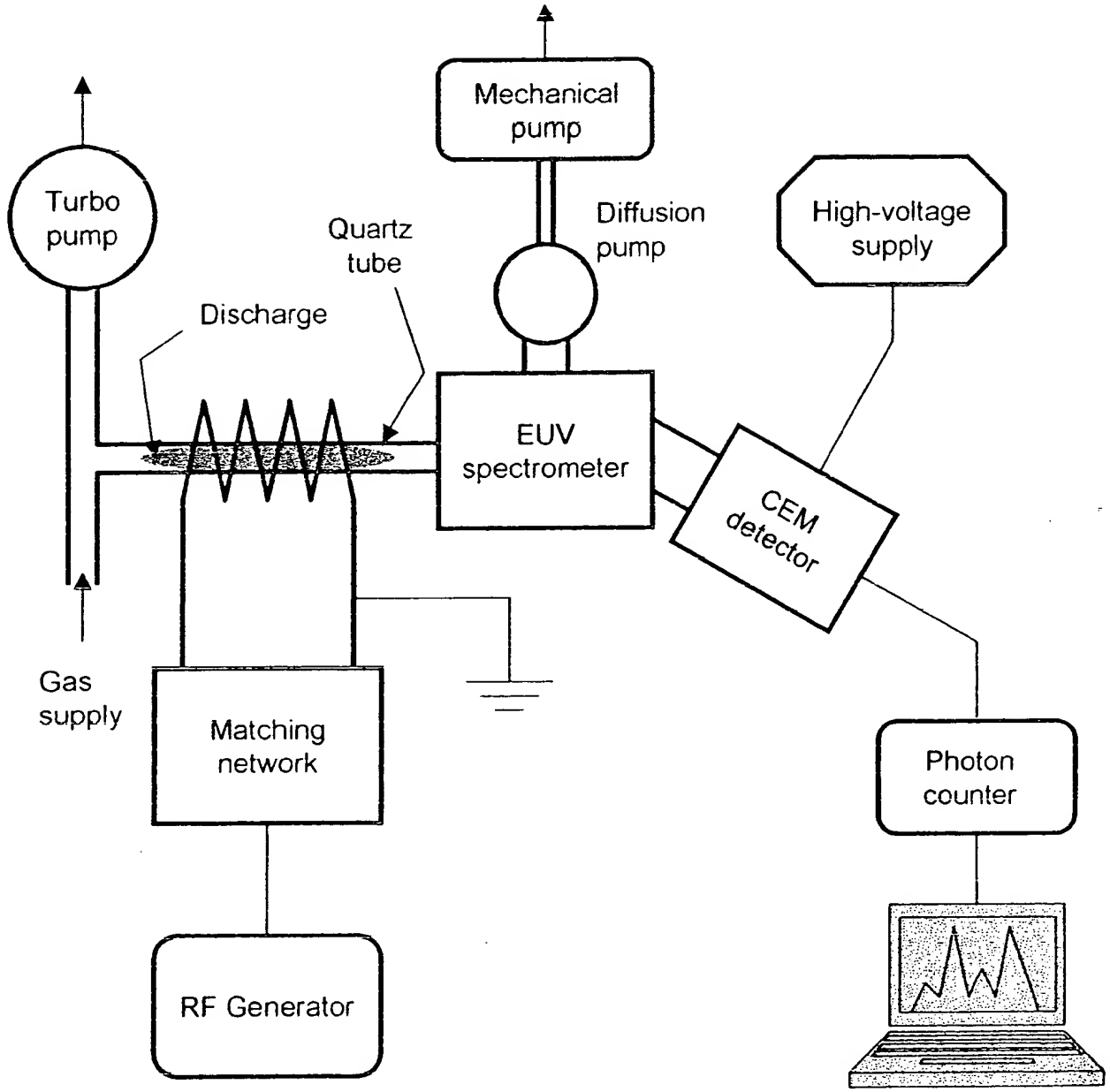
Mechanical pump
Turbo pump
Quartz tube
Diffusion pump
High-voltage supply
Discharge
EUV spectrometer
CEM detector
Gas supply
Matching network
Photon counter
RF Generator

Fig. 4

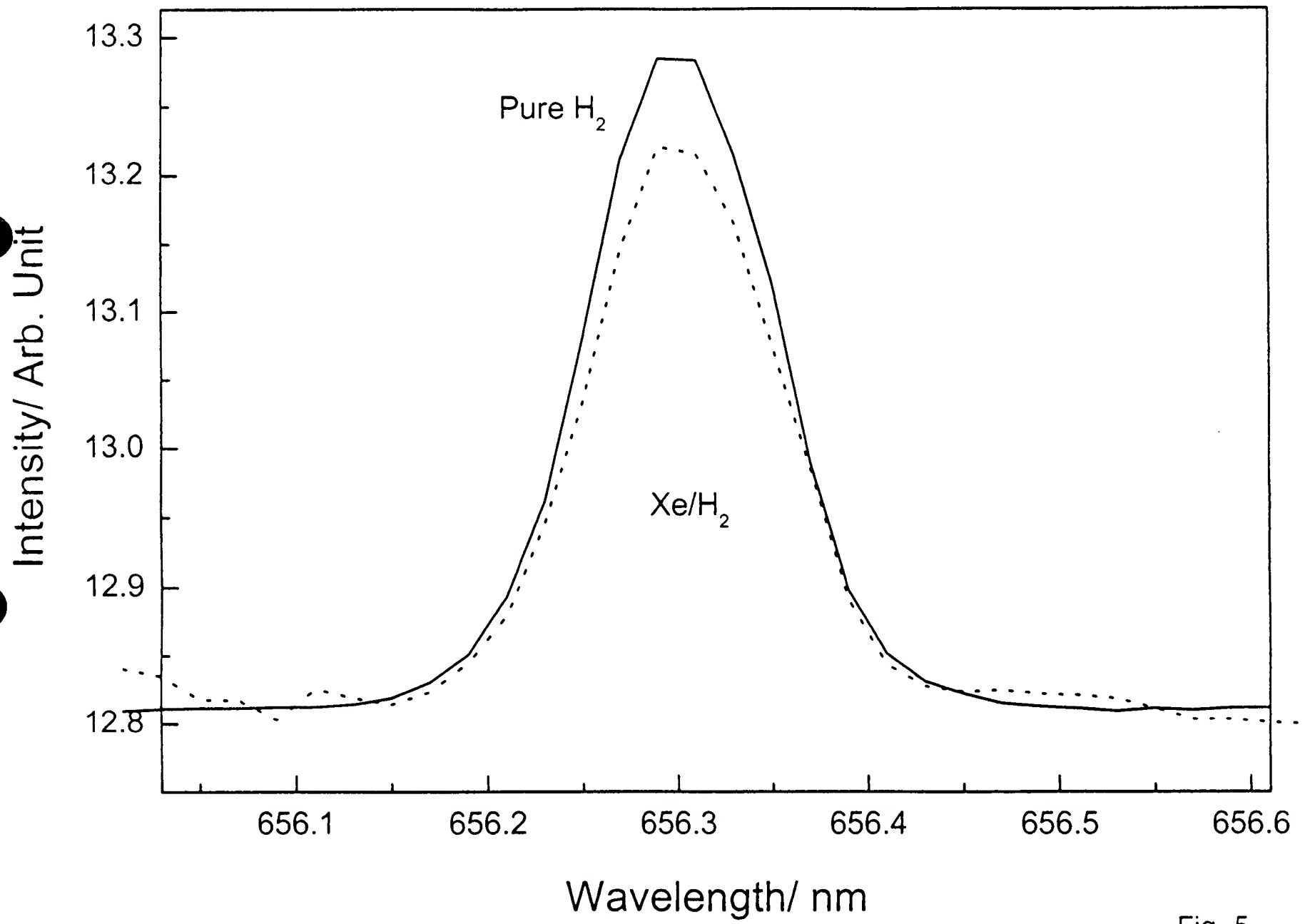
13.3
13.2
13.1
13.0
12.9
12.8
Intensity/ Arb. Unit
Pure $H_2$
$Xe/H_2$
656.1
656.2
656.3
656.4
656.5
656.6
Wavelength/ nm

Fig. 5

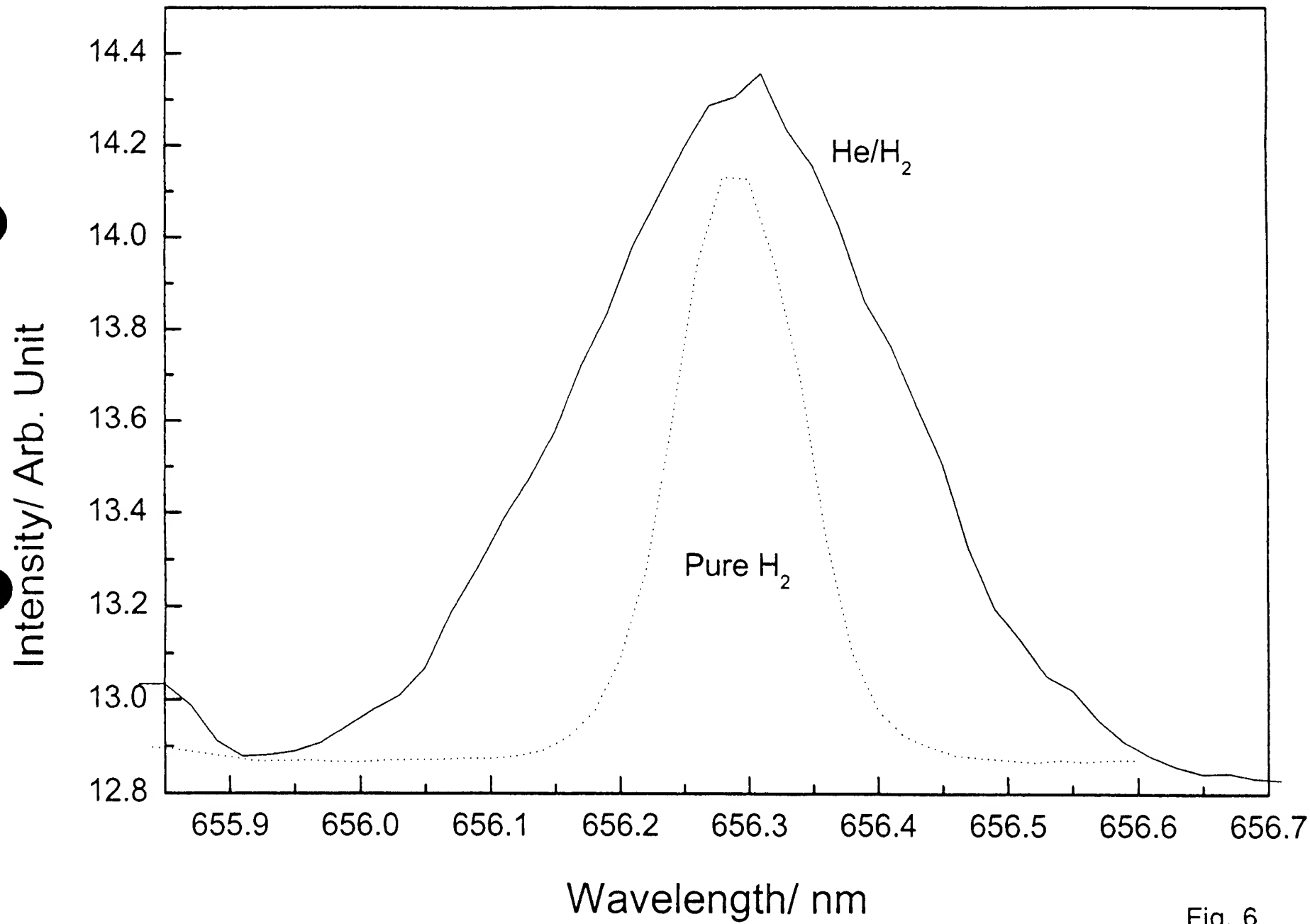
14.4
14.2
14.0
13.8
13.6
13.4
13.2
13.0
12.8
Intensity/ Arb. Unit
He/H2
Pure H2
655.9
656.0
656.1
656.2
656.3
656.4
656.5
656.6
656.7
Wavelength/ nm

Fig. 6

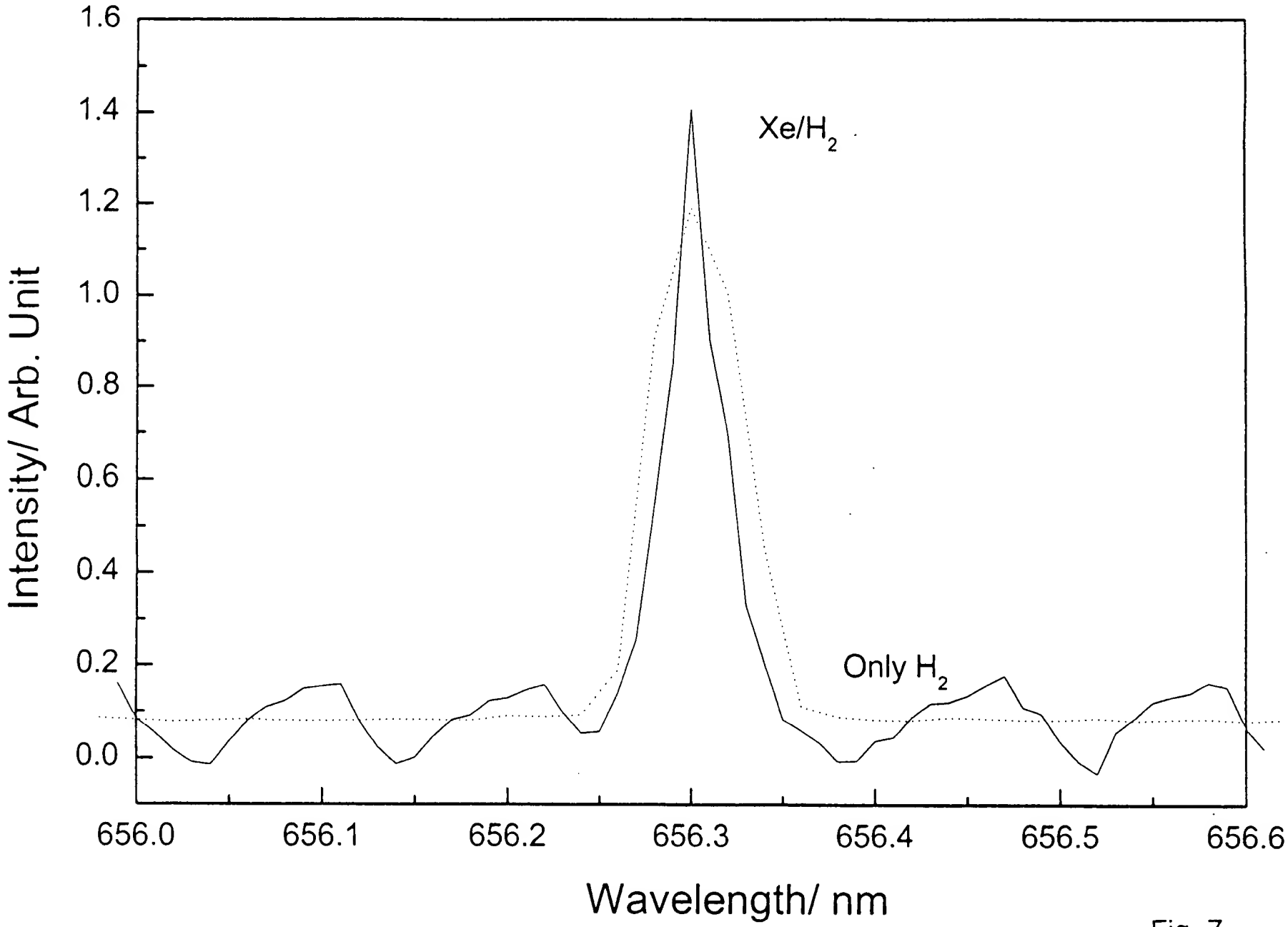
1.6
1.4
1.2
1.0
0.8
0.6
0.4
0.2
0.0
Intensity/ Arb. Unit
Xe/H2
Only H2
656.0
656.1
656.2
656.3
656.4
656.5
656.6
Wavelength/ nm

Fig. 7

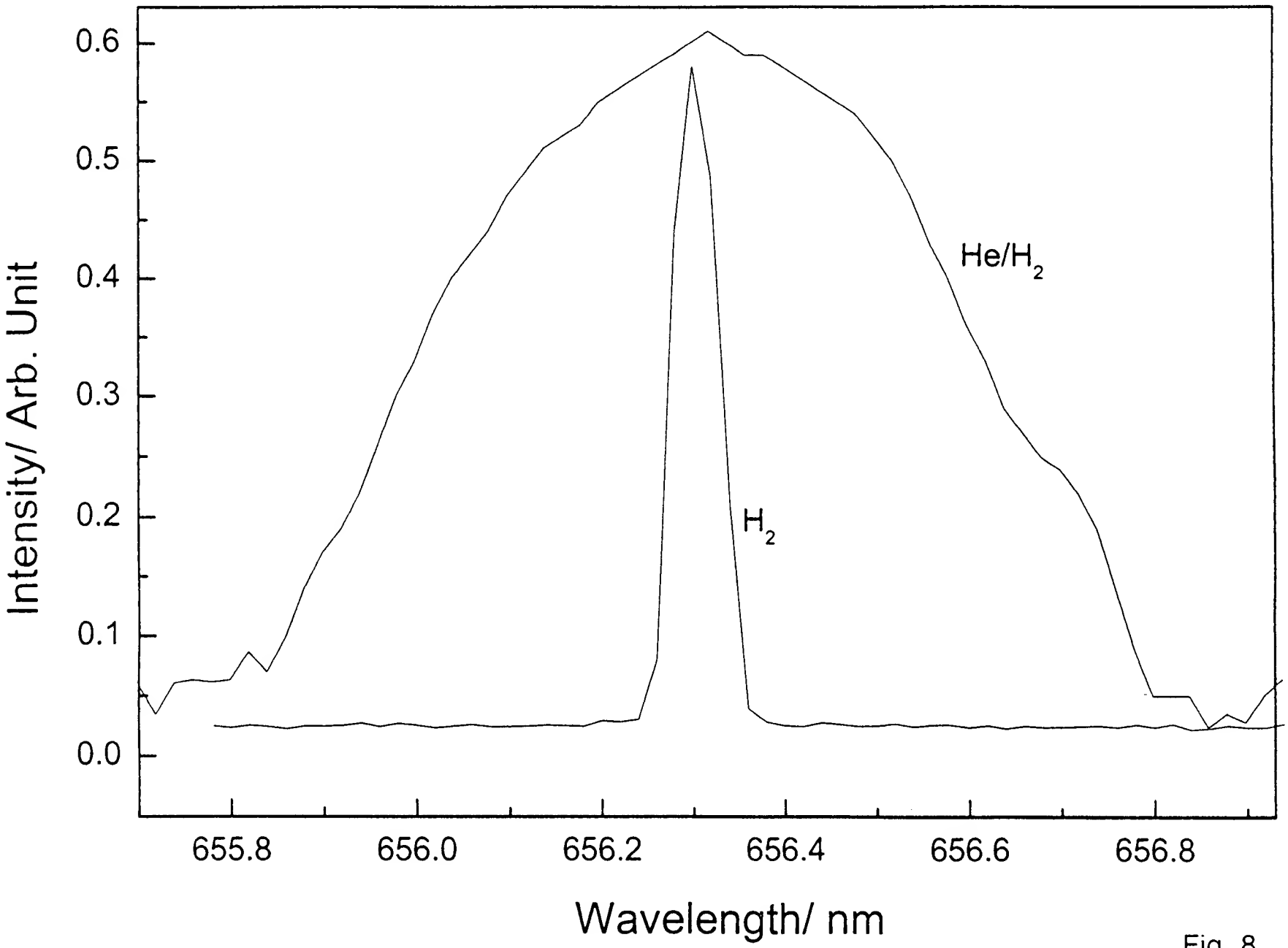
0.6
0.5
0.4
0.3
0.2
0.1
0.0
Intensity/ Arb. Unit
He/H2
H2
655.8
656.0
656.2
656.4
656.6
656.8
Wavelength/ nm

Fig. 8

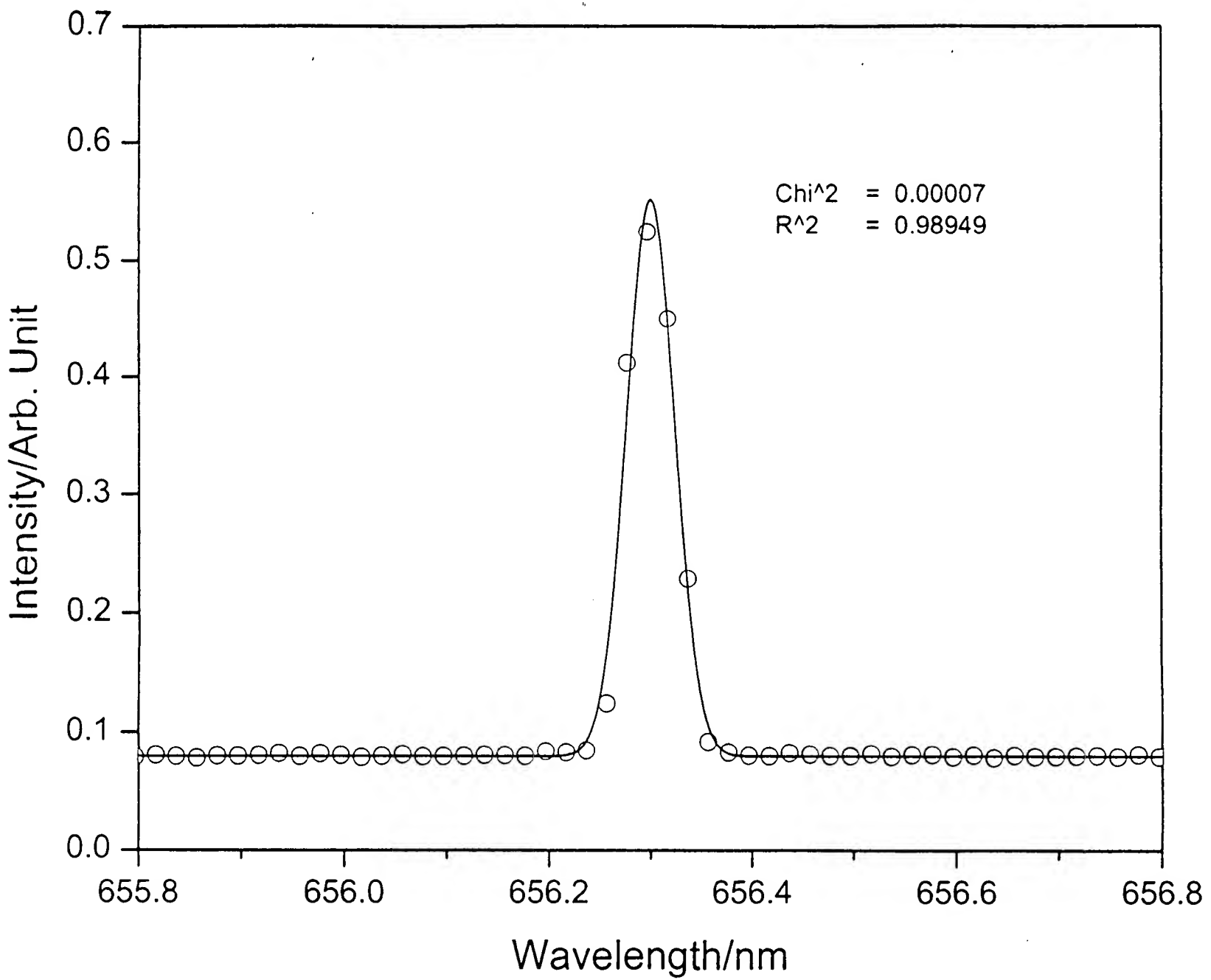
0.7
0.6
0.5
0.4
0.3
0.2
0.1
0.0
Intensity/Arb. Unit
Chi^2 = 0.00007
R^2 = 0.98949
655.8
656.0
656.2
656.4
656.6
656.8
Wavelength/nm

Fig. 9

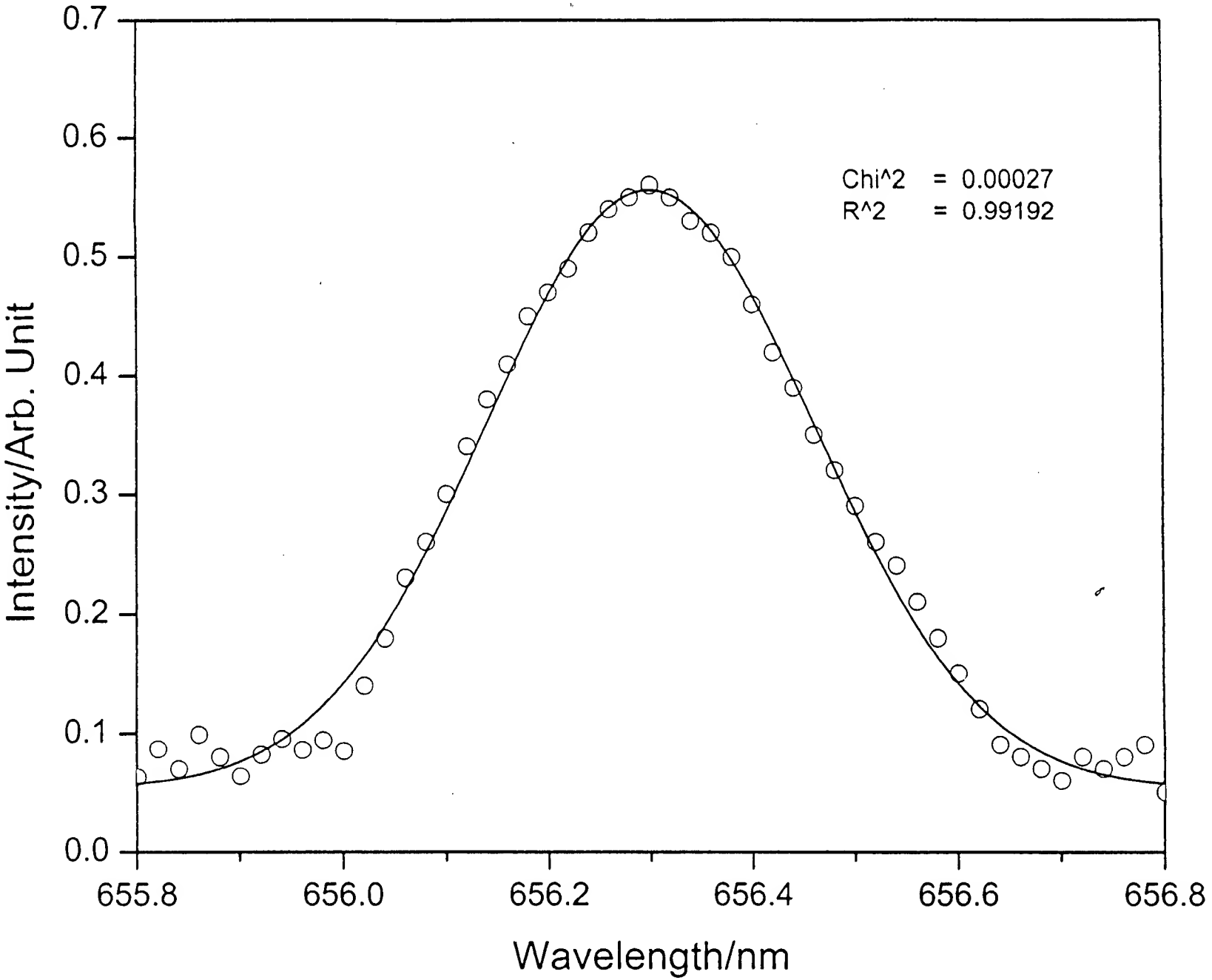
0.7
0.6
0.5
0.4
0.3
0.2
0.1
0.0
Intensity/Arb. Unit
Chi^2 = 0.00027
R^2 = 0.99192
655.8
656.0
656.2
656.4
656.6
656.8
Wavelength/nm

Fig. 10

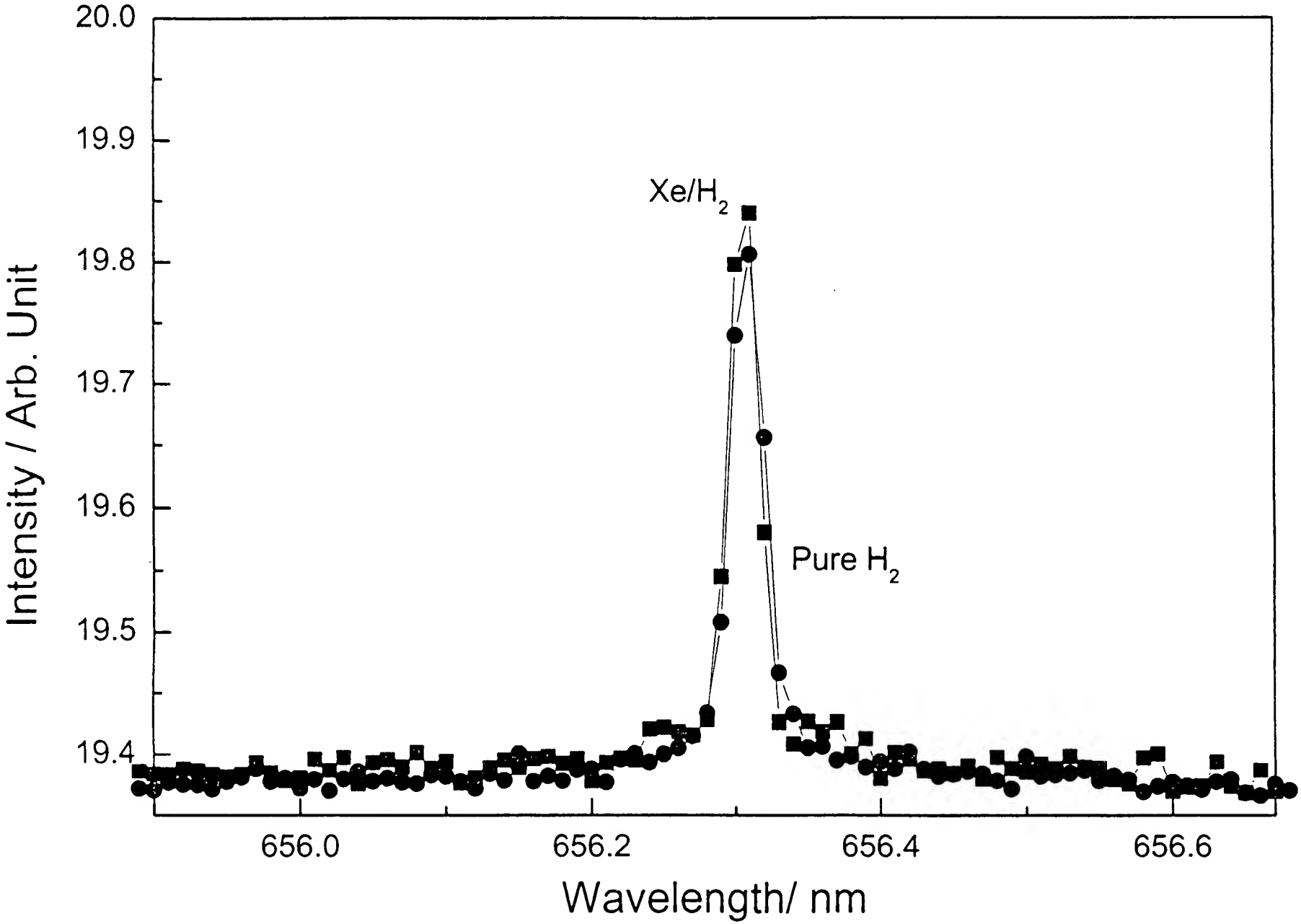
20.0
19.9
19.8
19.7
19.6
19.5
19.4
Intensity / Arb. Unit
Xe/H2
Pure H2
656.0
656.2
656.4
656.6
Wavelength/ nm

Fig. 11

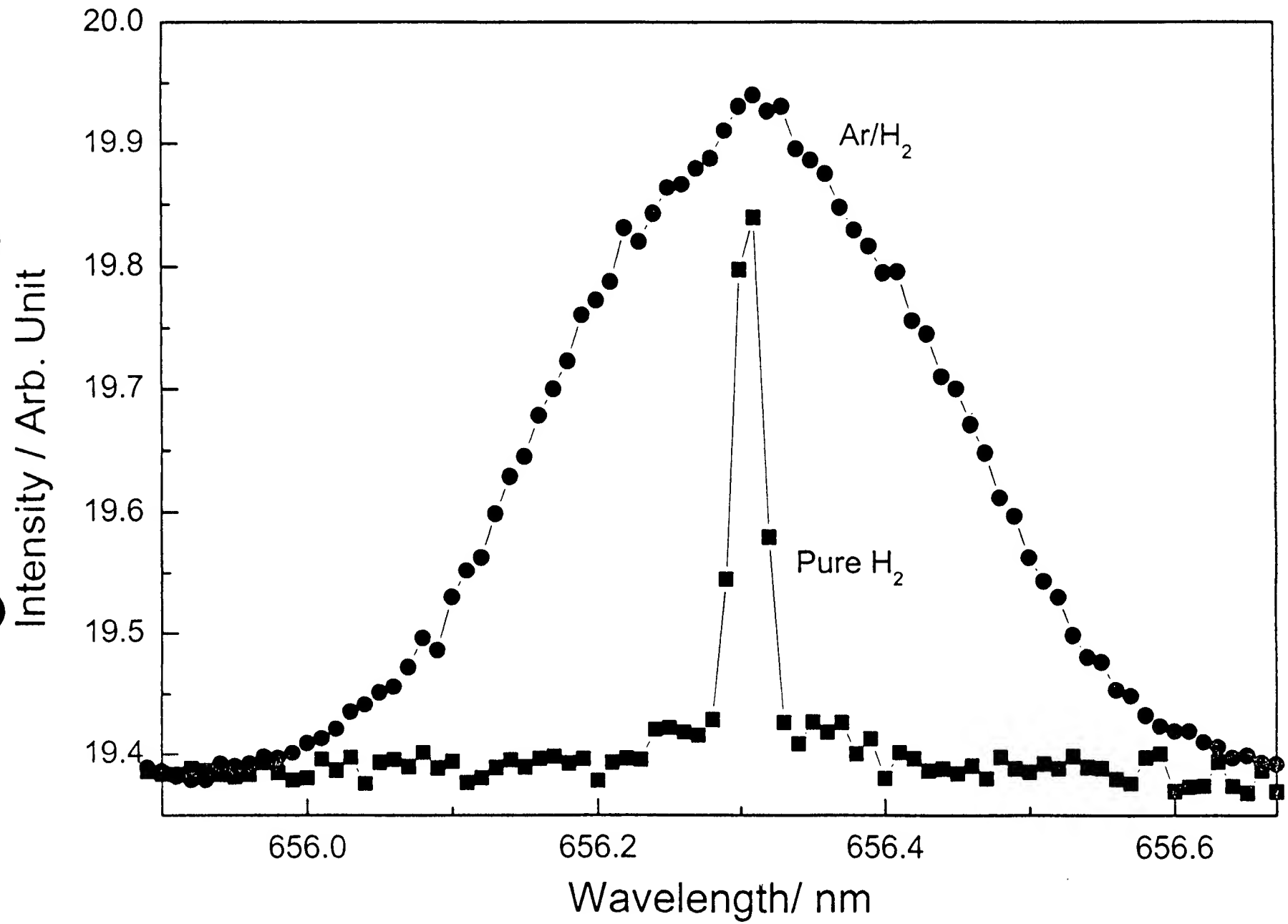
20.0
19.9
19.8
19.7
19.6
19.5
19.4
Intensity / Arb. Unit
Ar/H2
Pure H2
656.0
656.2
656.4
656.6
Wavelength/ nm

Fig. 12

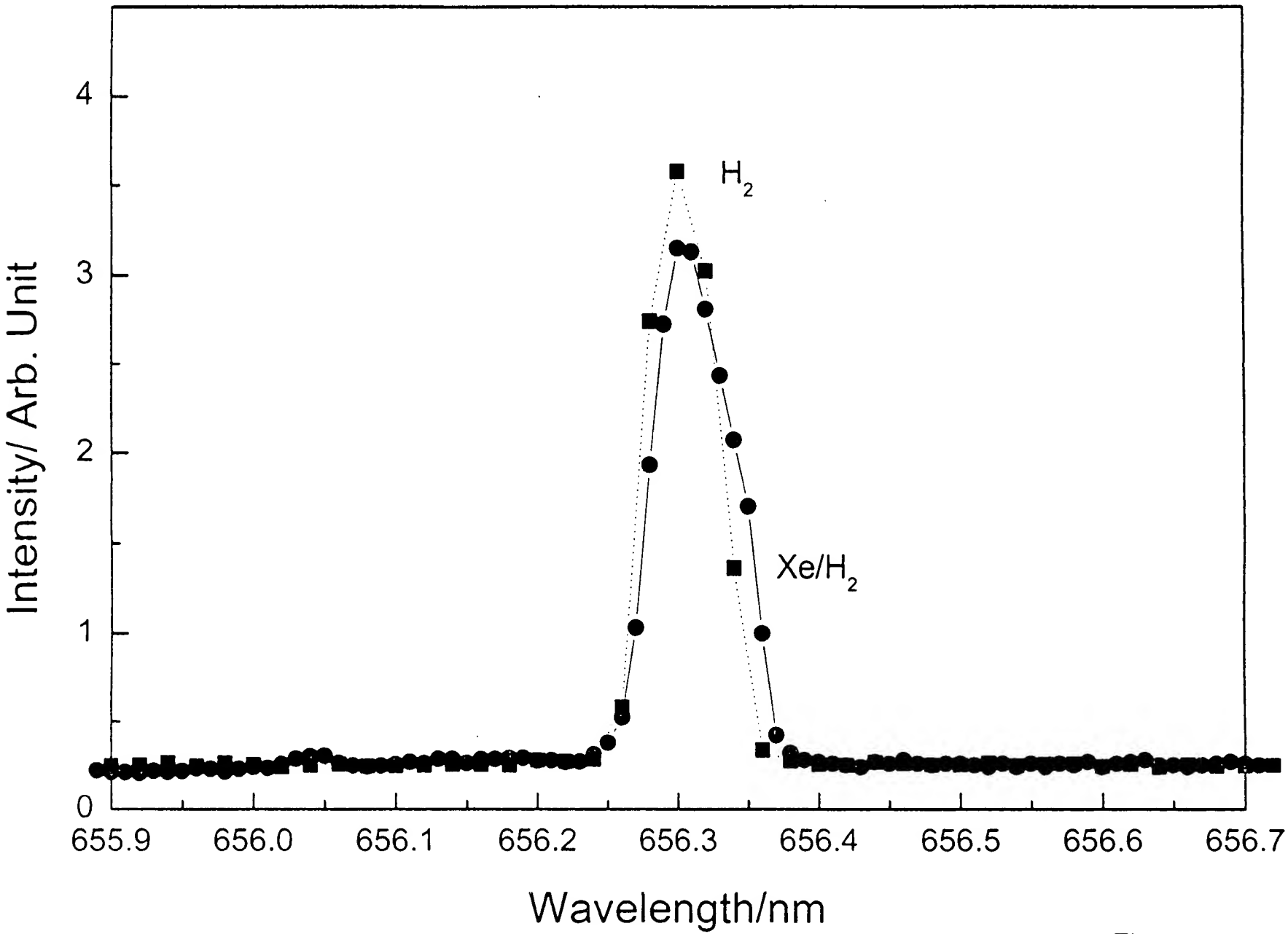
Intensity/ Arb. Unit
Wavelength/nm
H2
Xe/H2
0
1
2
3
4
655.9
656.0
656.1
656.2
656.3
656.4
656.5
656.6
656.7

Fig. 13

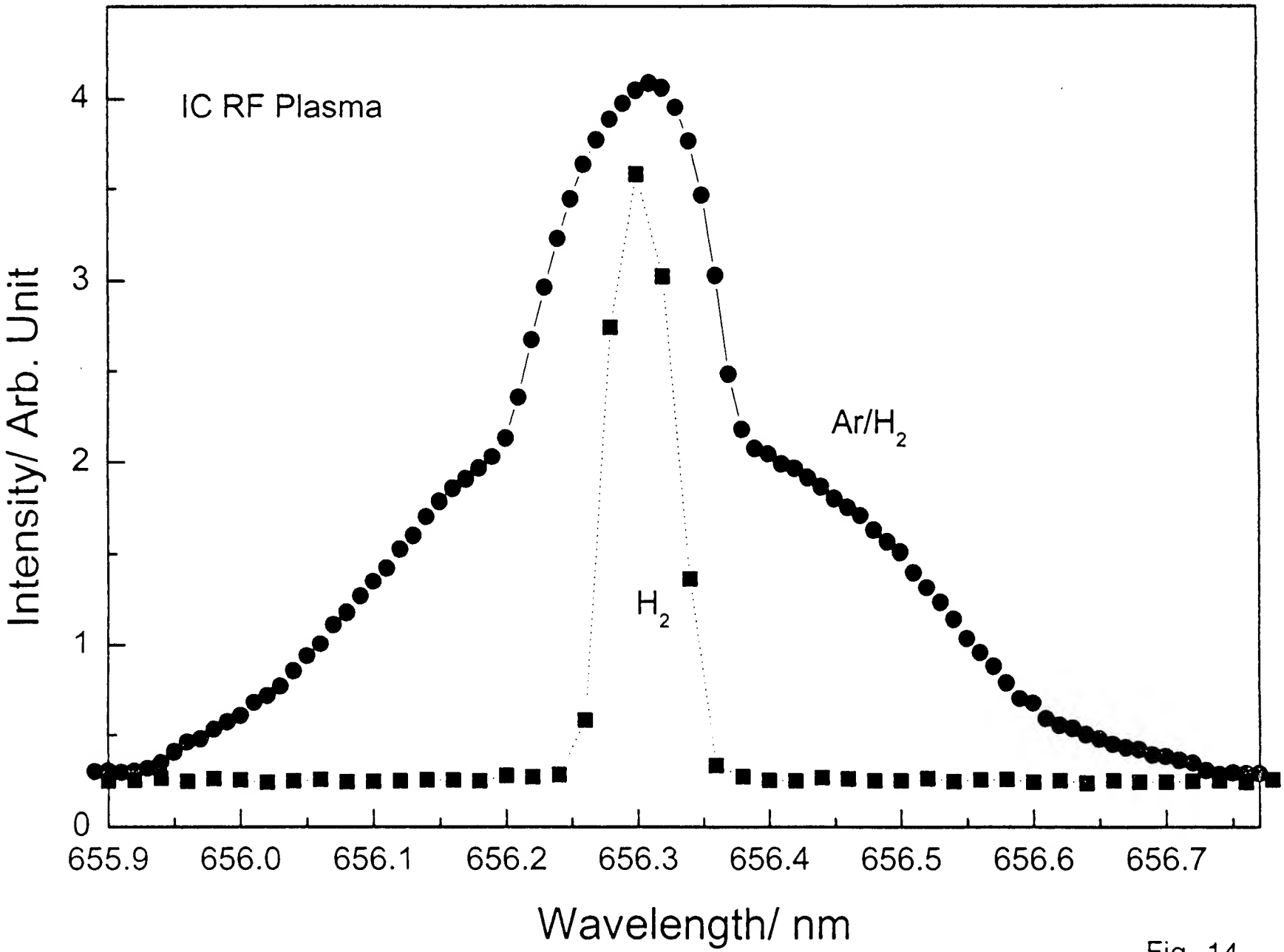
IC RF Plasma
Intensity/ Arb. Unit
Wavelength/ nm
Ar/H2
H2
0
1
2
3
4
655.9
656.0
656.1
656.2
656.3
656.4
656.5
656.6
656.7

Fig. 14

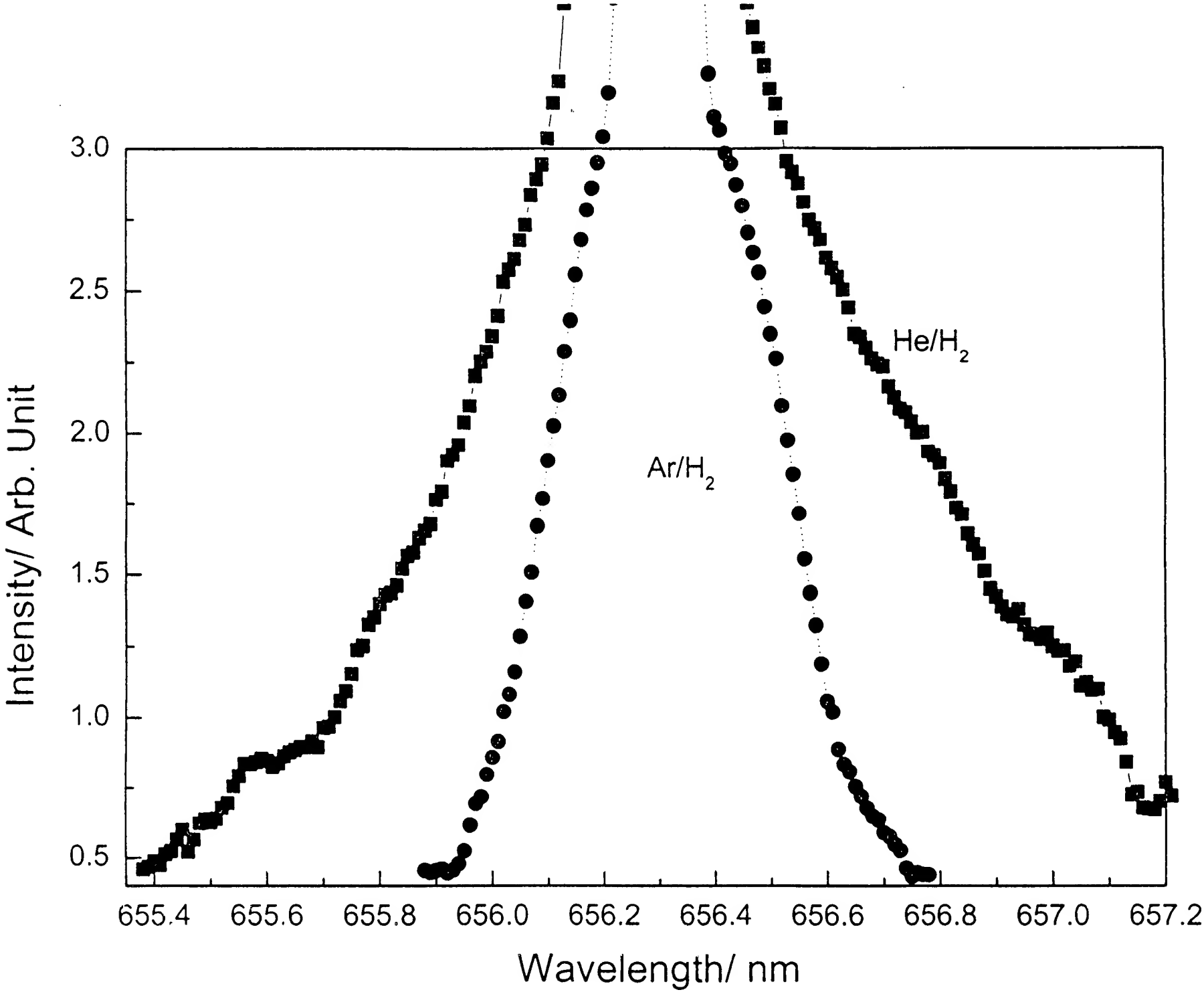
3.0
2.5
2.0
1.5
1.0
0.5
Intensity/ Arb. Unit
He/H2
Ar/H2
655.4
655.6
655.8
656.0
656.2
656.4
656.6
656.8
657.0
657.2
Wavelength/ nm

Fig. 15

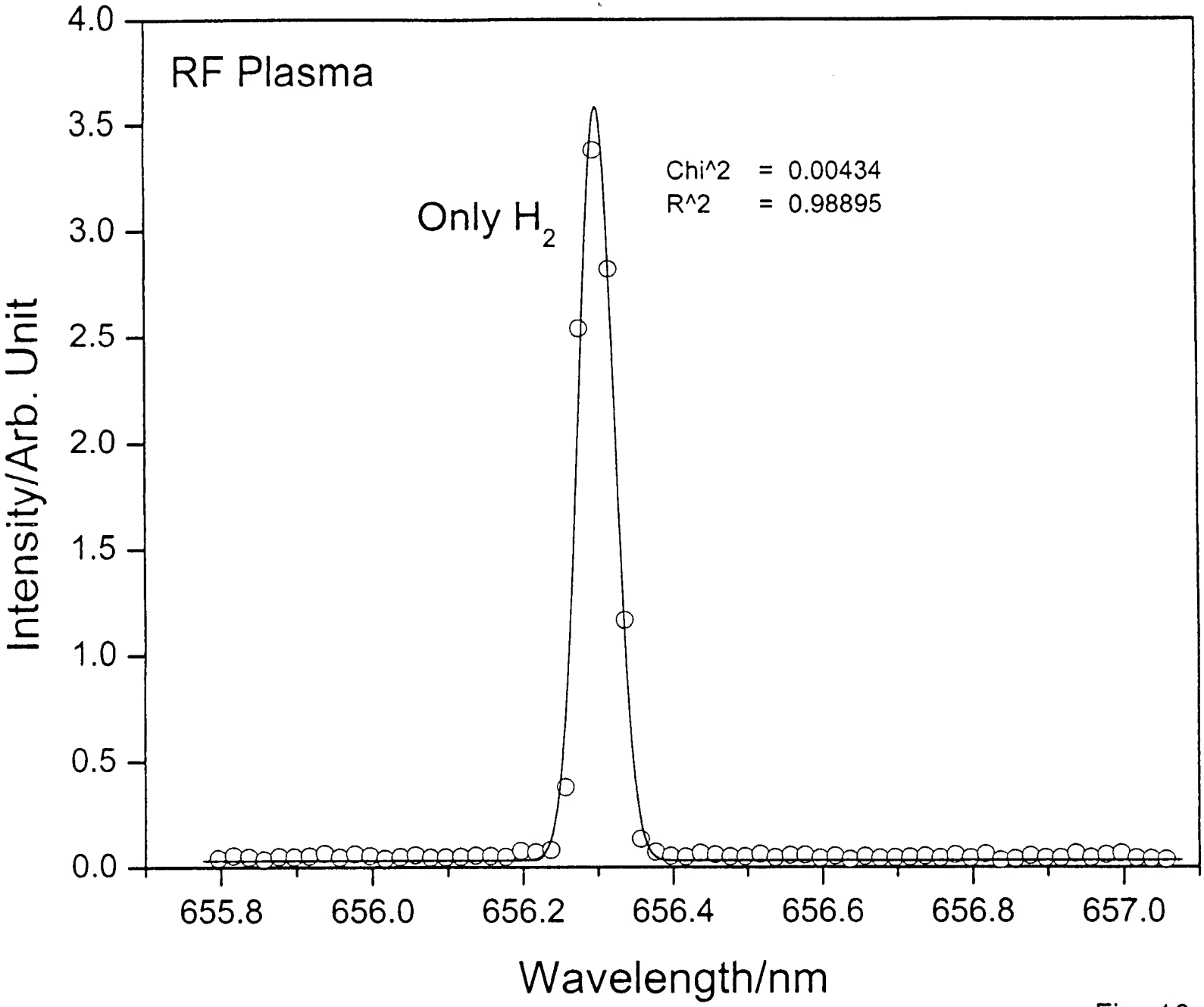
RF Plasma
Only $H_2$
Chi^2 = 0.00434
R^2 = 0.98895
Intensity/Arb. Unit
Wavelength/nm
4.0
3.5
3.0
2.5
2.0
1.5
1.0
0.5
0.0
655.8
656.0
656.2
656.4
656.6
656.8
657.0

Fig. 16

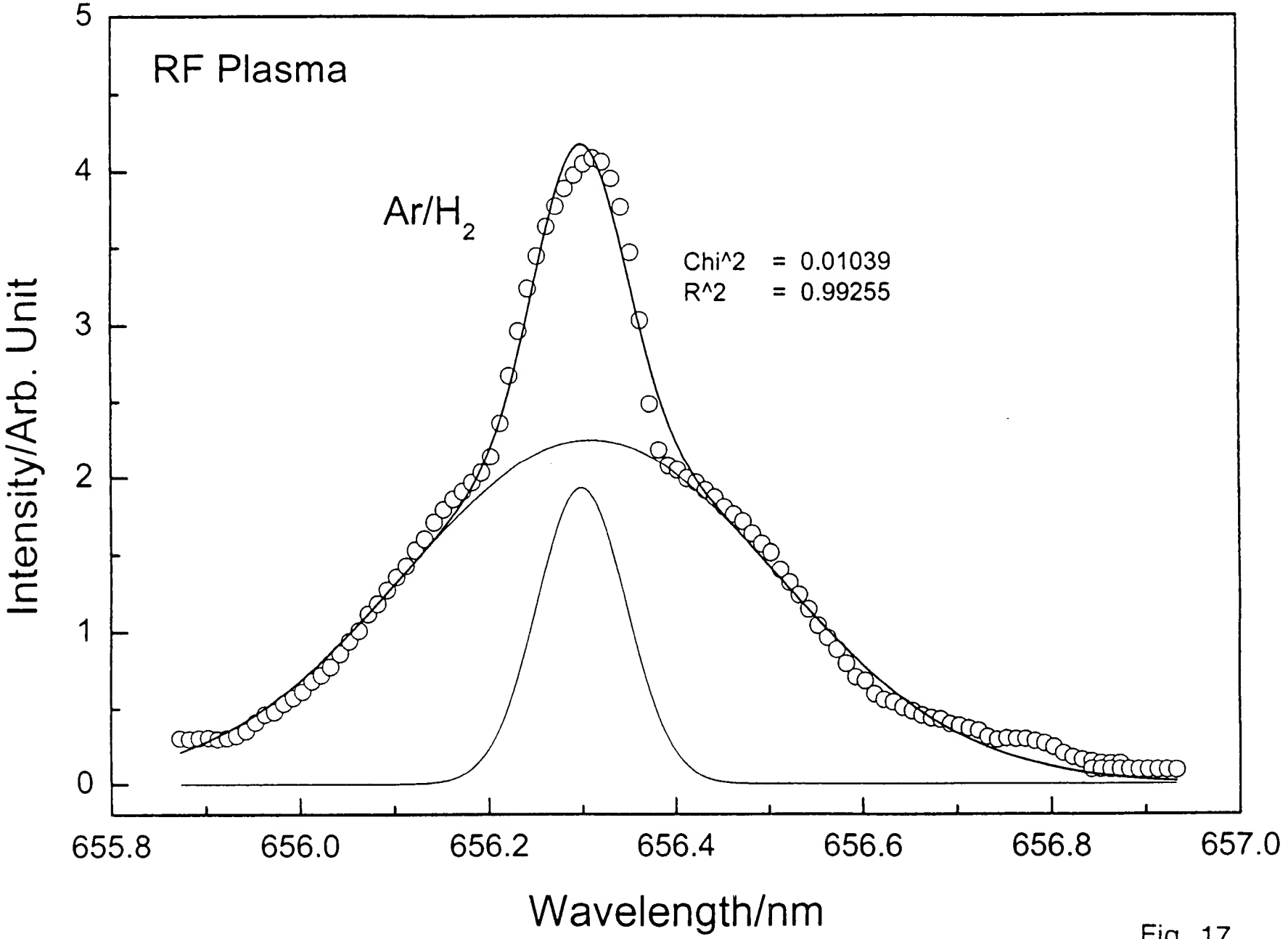
RF Plasma
Ar/H2
Chi^2 = 0.01039
R^2 = 0.99255
Intensity/Arb. Unit
Wavelength/nm
0
1
2
3
4
5
655.8
656.0
656.2
656.4
656.6
656.8
657.0

Fig. 17